

rel date 7/1/91

SBIR 09.10-1504

GRAPHITE-ALUMINUM COMPOSITES  
IN  
ADVANCED SPACE RADIATORS  
SBIR PHASE II

Contract NAS9-17806

## FINAL REPORT

11-10-10  
183165

P-83

Prepared for:

NATIONAL AERONAUTICS AND SPACE ADMINISTRATION  
LYNDON B. JOHNSON SPACE CENTER  
HOUSTON, TX 77053

COTR: W. RUSS LONG  
JOHN THORNBORROW

This SBIR data is furnished with SBIR rights under NASA Contract No. NAS9-17806. For a period of 2 years after acceptance of all items to be delivered under this contract the Government agrees to use this data for Government purposes only, and it shall not be disclosed outside the Government (including disclosure for procurement purposes) during such period without permission of the Contractor, except that, subject to the foregoing use and disclosure prohibition, such data may be disclosed for use by support Contractors. After the aforesaid 2-year period, the Government has a royalty-free licence to use, and to authorize others to use in its behalf, this data for Government purposes, but is relieved of all disclosure prohibitions and assumes no liability for unauthorized use of this data by third parties. This notice shall be affixed to any reproductions of this data, in whole or in part.

Prepared by:

Timothy A. Loftin

DWA COMPOSITE SPECIALTIES, INC.  
21119 Superior Street  
Chatsworth, CA 91311-4393

ORIGINAL PAGE IS  
OF POOR QUALITY

(NASA-CR-194231) GRAPHITE-ALUMINUM  
COMPOSITES IN ADVANCED SPACE  
RADIATORS Final Report (DWA  
Composite Specialties) 83 p

N94-70557

Unclass

## Project Summary

The objective of DWA Composite Specialties, Inc., in this second phase SBIR program was to fabricate a full-scale space radiator built around an experimental folding heat pipe supplied by Thermocore, Inc., of Lancaster, PA. The radiator framework and radiating panels had a mass of 1.5 Kg per meter (1 pound per foot) of radiator length, utilizing 16 square meters of tapered graphite-aluminum panel.

This effort grew out of a successful Phase I SBIR program investigating the application of high thermal conductivity metal matrix composite materials to space radiators. Results of analysis conducted in the Phase I effort indicated that thermal transfer per unit mass of radiator could be improved by approximately 17% by substituting a high thermal conductivity graphite-aluminum metal matrix composite (MMC) for conventional aluminum in radiating surfaces.

DWA fabricated the internal support structure around the heat pipe and assembled a series of graphite-aluminum panels into a lenticular section radiator of monocoque construction. The lenticular section was about 32mm (1.25 inch) deep in the center tapering to about 2mm (.06 inch) at the edges.

The active radiator was approximately 13.5 meters (44 feet) by 0.6 meter (2 feet). MMC surfaces were applied to both sides of the heat pipe.

The thermal transfer rate per unit mass was optimized by fabricating the MMC radiator skins themselves with a tapered cross section, varying in thickness from 0.63mm (.025 inch) at the center to 0.20mm (.008 inch) at the outer edges. The profile of the taper was the result of an analysis by Dr. Eugene Ungar of NASA Johnson Space Center. The analysis determined the taper required to maintain a constant thermal flux density through the radiator from the root to the outer edge. His analysis indicated that a 30% weight savings could be achieved without sacrificing thermal transfer rate.

The graphite-aluminum panels were fabricated by consolidating a set of plies of uniform thickness and varying widths approximating the profile specified by Dr. Ungar. The minimum ply thickness available through DWAs manufacturing process is approximately 0.13mm (.005 inches). The panels therefore consisted of 5 layers of graphite-aluminum stacked to form the required profile. All the graphite in the panels was aligned with the fibers perpendicular to the heat pipe. This orientation of fibers resulted in the maximum thermal conductivity away from the heat pipe.

In addition to the construction of the radiator, a series of thermal transfer performance and thermal conductivity measurements were made. DWA constructed a small thermo-vacuum chamber with a liquid nitrogen-cooled cold wall. Six specimens were tested: copper, aluminum, tapered unidirectional graphite-aluminum, constant thickness unidirectional graphite-aluminum (in both orientations), 0-90 cross-plyed graphite-aluminum and ~~±45 cross-plyed graphite-aluminum~~. The thermal conductivity of the same materials was measured. For the anisotropic composite materials, the conductivity was measured in three orthogonal directions.

Of the six panels tested, the highest transfer rate per unit of mass in the given geometry was provided by the tapered graphite aluminum at 186 watts per Kg. The lowest was copper at 12 watts per Kg.

The mass loss in graphite-aluminum resulting from exposure to high vacuum for one week was measured to be 0.002 percent.

The experience of this effort indicates that the cost of such a high-performance graphite-aluminum radiator can completely recovered by savings in launch costs resulting from reduced weight..

## Table of Contents

Section	Title	Page
	Forward .....	3
	LENTICULAR SECTION RADIATOR .....	4
1.0	RADIATOR DESIGN .....	4
1.1	Resonant Frequency Considerations .....	4
1.2	Heat Pipe Design .....	9
1.3	Composite Thermal Conductivity and Thermal Transfer .....	13
1.3.1	Measurement Technique: Thermal Conductivity .....	14
1.3.2	Results of Thermal Conductivity Measurements .....	18
1.3.3	Measurement Technique: Radiative Transfer .....	21
1.3.4	Results of Radiative Thermal Transfer Measurements .....	26
1.4	Radiator Panel Configuration .....	26
1.5	Radiator Structure .....	28
2.0	RADIATOR FABRICATION .....	35
2.1	Fabricate Graphite-Aluminum Panels .....	42
2.2	Fabricate Braces and End-Caps .....	44
2.3	Fabricate Assembly Jigs and Fixtures .....	44
2.3.1	Radiator Frame Cradle .....	51
2.3.2	Radiator Frame Table .....	51
2.3.3	Panel Pressure Plate .....	51
2.3.4	Panel Radius Forming Tool .....	51
2.4	Attach Braces and End-Caps to Heat Pipe .....	57
2.5	Attach Graphite-Aluminum panels to Radiator Frame .....	57
3.0	SUMMARY, CONCLUSIONS AND RECOMMENDATIONS .....	62
3.1	Summary .....	62
3.2	Conclusions .....	65
3.2.1	Manufacturing Technology .....	66
3.2.2	Radiator Cost .....	66
3.2.3	Radiator Weight .....	67
3.3	Recommendations .....	67
	Vibrations in Composite Beams .....	APPENDIX 1
	High Thermal Conductivity Filled Epoxy .....	APPENDIX 2
	Structural Epoxy .....	APPENDIX 3

## List of Tables

1	Radiative Transfer Test Panels .....	15
2	Thermal Conductivity Measurements .....	20
3	Radiative Transfer Test Results .....	27

No.	Title	Page
1	Folding Lenticular Section Radiator .....	5
2	Resonant Vibration Mode .....	6
3	Box-Beam Stiffened Radiator .....	7
4	Radiator Representative Sections .....	8
5	Monogroove Heat Pipe Section .....	10
6	Lenticular Radiator Section .....	11
7	Thermocore Heat Pipe Section .....	12
8	Radiative Transfer Test Panels .....	16
9	In-plane Thermal Conductivity Measurement .....	17
10	Thru-plane Thermal Conductivity Measurement .....	19
11	Thermovacuum Chamber .....	22
12	Thermovacuum Chamber .....	23
13	Thermovacuum Chamber .....	24
14	Thermocouple Layout: Radiative Transfer Test .....	25
15	Tapered Radiator Thickness Profile .....	29
16	Tapered Radiator Temperature Profile .....	30
17	Stepped Radiator Thickness Profile .....	31
18	Radiator Panels Around Heat Pipe .....	32
19	Stepped Radiator With Aluminum-Rich Zone .....	33
20	Lenticular Section Radiator .....	34
21	Folding Heat Pipe .....	36
22	Radiator Brace .....	37
23	Radiator Edge-Cap .....	38
24	Radiator Brace Spacing .....	39
25	Edge-Cap to Brace Attachment .....	40
26	Edge-Cap Splice .....	41
27	Trial Lenticular Radiator Section .....	43
28	Sanded Gr-Al Panel .....	45
29	Seam in Graphite-Aluminum Panel at Heat Pipe .....	46
30	Layout of Radiator Panels .....	47
31	Waviness in Gr-Al Panels .....	48
32	Radiator Braces .....	49
33	Radiator Edge-Cap .....	50
34	Cradle Support .....	52
35	Cradle Platform .....	53
36	Platform Adjusting Screw .....	54
37	Frame Table .....	55
38	Pressure Plate .....	56
39	Heat Pipe in Cradle .....	58
40	Brace in Position .....	59
41	Weighted Pressure Plate .....	60
42	Wavy Gr-Al Panels .....	61
43	Reduced Length Panels .....	63
44	Ribbon Repairs .....	64

## Foreword

This contract grew out of a successful Phase I SBIR contract (No. NAS9-17571) completed in 1986 by DWA Composite Specialties, Inc., for the NASA Johnson Space Center in Houston, Texas. The Contracting Officers Technical Representative for the effort was Mr. W. Russ Long and the Principal Investigator for DWA was Mr. Timothy A. Loftin.

The first phase effort demonstrated that the improved thermal conductivity provided by high modulus graphite fibers in a matrix of aluminum could improve the thermal transfer rate of space radiators. By replacing aluminum skins with graphite-aluminum in the radiating structure, the thermal transfer rate could be improved by 17% with no weight penalty.

The initial goal of the 2-year second phase of the effort was to investigate configurations of composite materials selected to meet several design requirements for the thermal management radiators being developed for the Space Station. Weight, thermal transfer rate and resonant frequency for the radiating structure were design considerations against which radiator structural designs and composite material configurational designs were to be compared. It was expected that tradeoff decisions for structural stiffness and thermal transfer rate would require adjusting composite thickness and fiber orientation parameters. To provide data for these decisions, an extensive series of tests were outlined. The tests were to include thermal conductivity and mechanical property measurements for a large number of panels with varying thicknesses, fiber volume fractions and ply orientations. Thermal transfer performance for each configuration was to be measured in a cold-wall thermal vacuum chamber to be fabricated by DWA. The effort was to conclude with the construction of several large panels, approximately 0.6 meters by 1.5 meters (2 feet by 5 feet) in extent to be delivered to NASA for further testing.

Midway through the effort it was decided by mutual agreement between DWA and NASA that a more valuable goal would be the construction of a full scale article optimized for weight and thermal transfer. The contract was modified, eliminating the bulk of the test matrix and the loose panels to be fabricated and substituting the construction of a full-sized radiator using a heat-pipe supplied by NASA.

The thermal-vacuum chamber was constructed and a reduced set of tests were conducted. The tests included thermal conductivity, radiative thermal transfer performance and offgassing under vacuum.

The cost and period of performance of the contract were unaffected by the change.

Near the end of the contract the Mr. Long left NASA and was replaced by Mr. John Thornborrow as COTR.

## Lenticular Section Radiator

The radiator built by DWA for NASA JSC is shown in Figure 1 . It was built around a two-phase heat pipe constructed by Thermocore, Inc., of Lancaster, PA. A light-weight internal structure of formed aluminum sheet was built by DWA and attached to the heat pipe. The radiator was completed by attaching a series of graphite-aluminum panels to the top and bottom of the structure and heat pipe. The design and construction of the radiator is described in the sections following. The details of the fabrication of the graphite-aluminum panels are proprietary to DWA and are not included.

### 1.0 RADIATOR DESIGN

The radiator was designed to utilize an experimental heat pipe fabricated by Thermocore, Inc., of Lancaster, Pa, and to meet the following goals:

- transfer capacity : 2000 watts
- root temperature : 15°C (60°F)
- radiating length : 15 meters
- radiating width : 0.6 meters ( radiating 2 sides)
- weight : minimum
- resonant frequency : >0.10 Hz
- exposed edge radius: >1.5 mm (0.06 inch)

### 1.1 Resonant Frequency Considerations

After the determination of the radiator envelope, i.e., length, width and radiating area, a major constraint on the detail structural design of the radiator is the requirement for a natural resonant frequency greater than 0.1 hz in the vibration mode depicted in Figure 2.

Preliminary calculations performed by other contractors for NASA JSC indicated that achieving the structural stiffness required to produce a resonant frequency in excess of the minimum would dictate the construction of a box-beam design as shown in Figure 3.

The primary objective of this program was to minimize the weight of a radiating structure. Accordingly, one of the early program tasks was to investigate methods of fabricating composite radiating panels with sufficiently high structural stiffness that the vibration requirement could be met with a minimum of weight. Four prospective radiator designs were considered and representative sections of each fabricated to identify manufacturing problems associated with each. The four section are shown in Figure 4. The designs investigated stiffening by box-beam construction and intrinsic

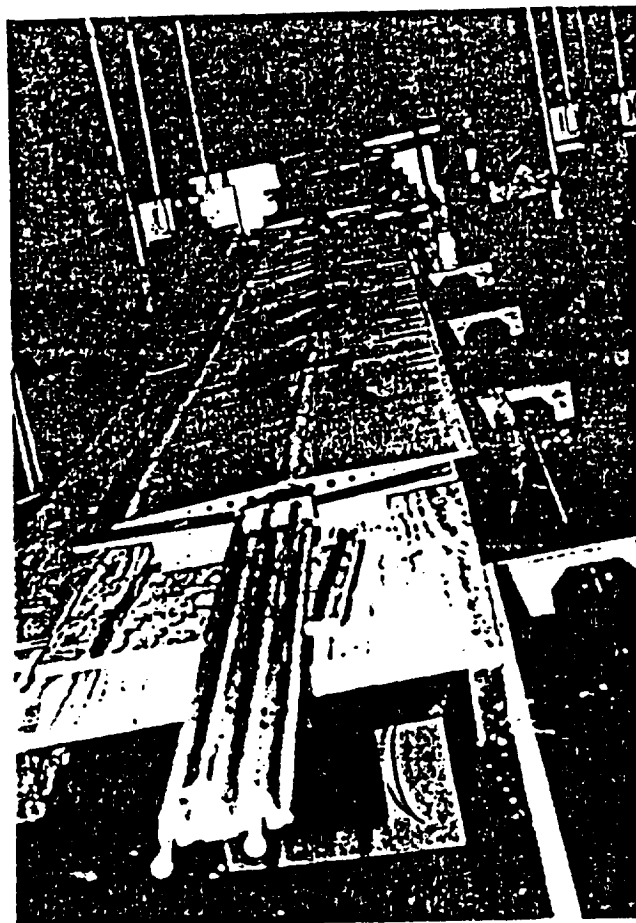


FIGURE 1  
Folding Lenticular Radiator

ORIGINAL PAGE IS  
OF POOR QUALITY

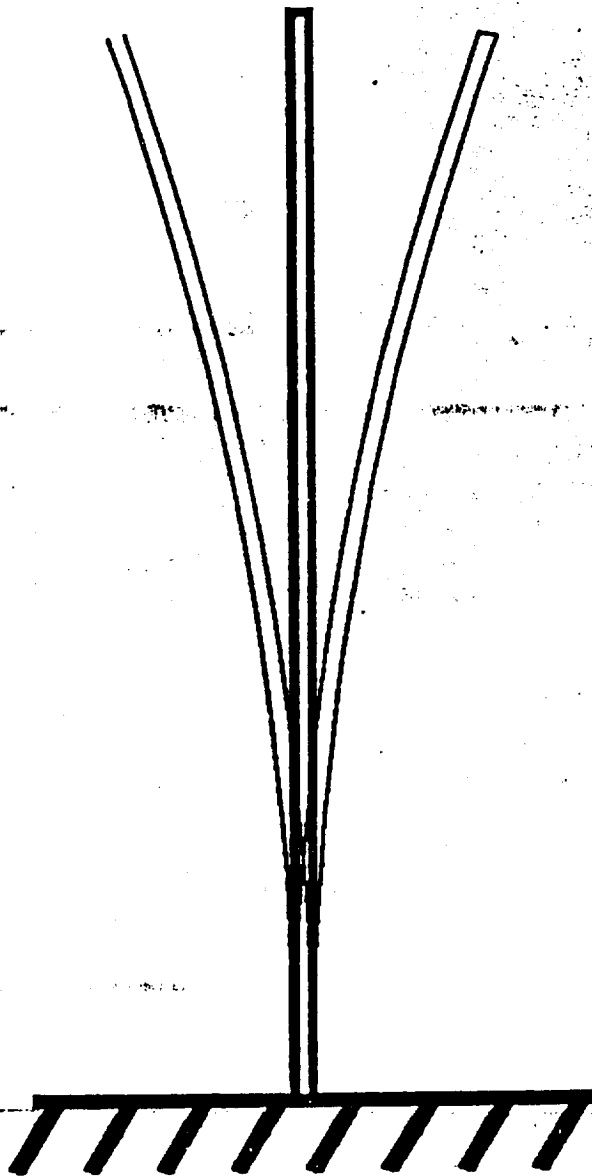


FIGURE 2  
Resonant Vibration Mode



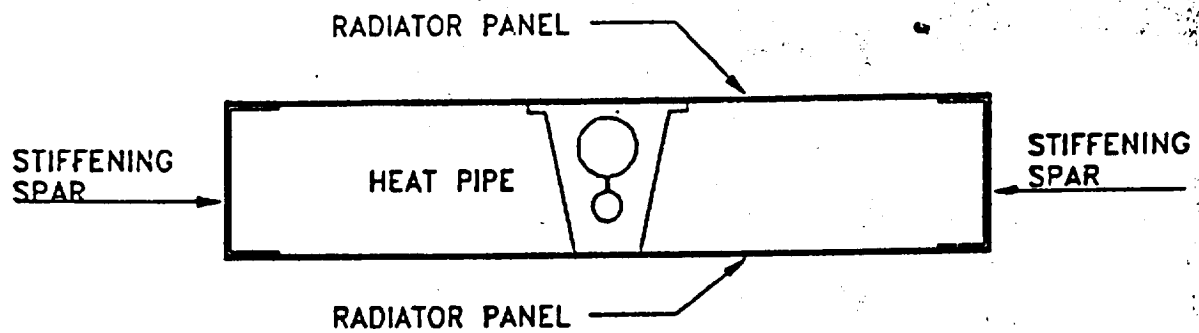
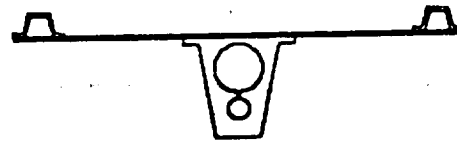


FIGURE 3  
Box-Beam Stiffened Radiator Design



A. BOX-BEAM STRUCTURE



B. EDGE STIFFENED



C. CENTRALLY STIFFENED



D. SELF-STIFFENED

FIGURE 4  
Representative Radiator Section Designs

stiffening of the panel itself.

The designs were also affected by the requirement to avoid any exposed edges with less than 1.5 mm radius of curvature (sharp edges being hazardous to space-suited astronauts).

The three sections labeled A, B and C were fabricated and delivered to NASA JSC. Each was built around a section of heat pipe supplied by NASA. The design of the heat pipe is shown in Figure 5. The section labeled D was not produced. In its place was fabricated a section representative of the final lenticular section shown in Figure 6. Its construction is described in Section 2.1.

At the outset of this effort, it was assumed that any radiator constructed of composite materials would need some version of box-beam construction to meet the vibration requirement. This assumption created the need to balance the lengthwise structural stiffness in the composite radiating panels with their transverse thermal conductivity. The first property requires fibers parallel to the heat pipe, the second requires fibers perpendicular to the heat pipe. Anticipating the need to evaluate different cross-plyed composite configurations against these conflicting structural and thermal requirements, an extensive matrix of material properties tests was designed. Panels of varying fiber orientation and panel thickness were to be fabricated and the thermal transfer characteristics of each measured as described below. The configuration offering the highest thermal transfer with the greatest lengthwise stiffness would be used in the design of the radiator.

Analyses performed at NASA and at DWA during the evaluations of potential designs showed that the original resonant frequency calculations were in error and that a box-beam construction was not needed to meet the 0.1 Hz requirement (Appendix I). A simple aluminum plate attached to the heat pipe was sufficiently stiff. The thermally optimal composite design, with all graphite fibers parallel to the heat pipe was also sufficiently stiff. This conclusion removed the necessity for the trade-off study using the test matrix described above. This fact influenced the later decision to change the objective of the contract from data generation to full scale hardware fabrication. In the radiator constructed, all fibers were arranged for optimal thermal transfer, with no special consideration for lengthwise stiffness.

## 1.2 Heat Pipe Design

The central component in the construction of the radiator was an experimental folding heat pipe fabricated for NASA JSC by Thermocore, Inc. The heat pipe was fabricated in three sections, each with approximately 4.5 of two-phase heat pipe linked by flexible hoses joining the vapor and fluid arteries. An evaporator assembly was attached to one end, absorbing energy from an external thermal management system and transporting through the length of the heat pipe. The total length of the heat pipe was approximately 17.4 meters, folding into a length of approximately 5.3 meters.

The heat pipe was circular in cross section, with an internal structure shown in Figure 7.

The heat pipe was received with damage incurred in shipment. One end of the wooden crate containing the heat pipe was crushed and appeared to have been punctured by the tines of a forklift.

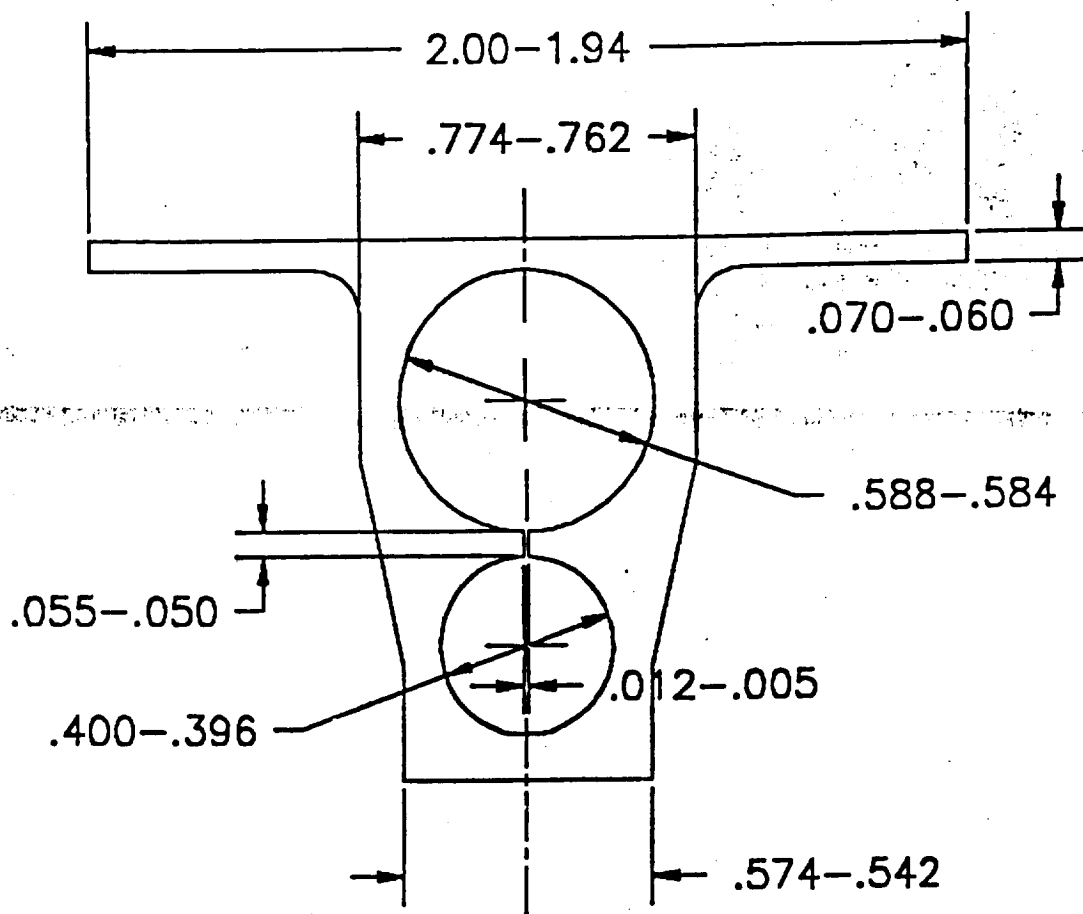


FIGURE 5  
Monogroove Heat Pipe Section

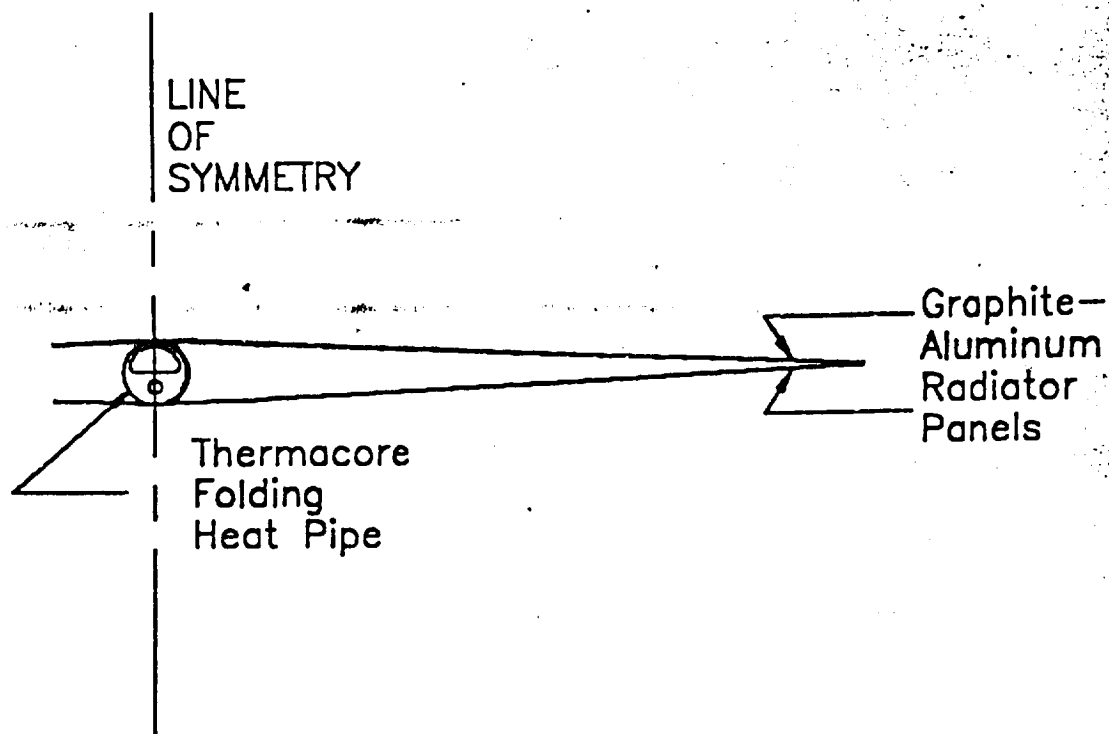


FIGURE 6  
Lenticular Section Radiator

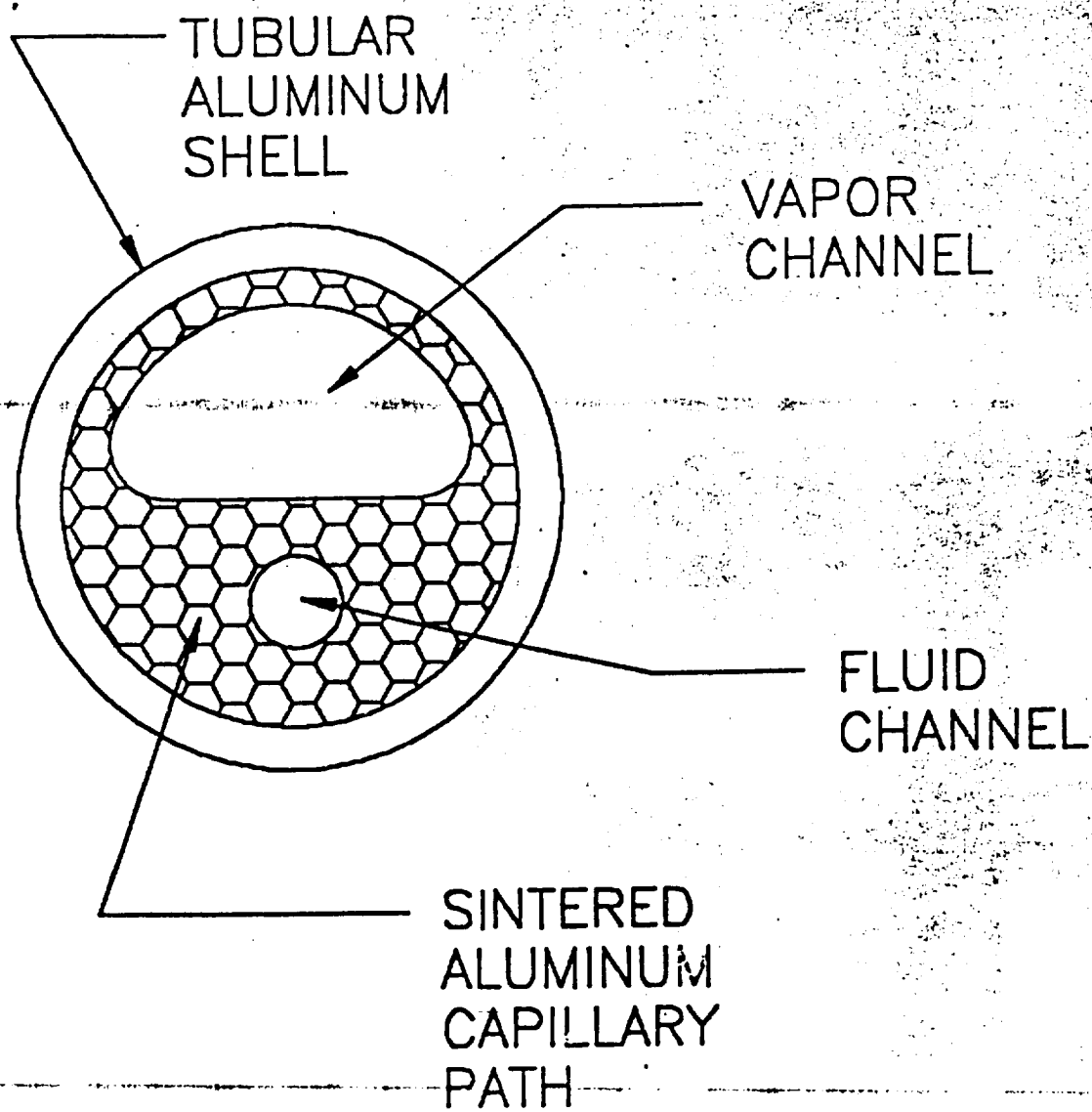


FIGURE 7  
Thermocore Heat Pipe Section

ORIGINAL PAGE IS  
OF POOR QUALITY

The heat pipe itself had several feed tubes welded to the evaporator assembly, located at the damaged end of the crate. One of the feed tubes had been bent downward and the weldment cracked. The working fluid in the heat pipe had been lost.

### 1.3 Composite Thermal Conductivity and Thermal Transfer

The primary function of the skins in a thermal management radiator is to provide a conductivity path away from the heat pipe, spreading the thermal energy over a large area for effective transfer by radiation. The most efficient radiator provides maximum thermal conductivity perpendicular to the heat pipe; in a long radiator with a uniform root temperature, there is no heat transferred parallel to the heat pipe in the radiating skin. Theoretically, thermal conductivity in this direction could be zero with no loss of thermal transport capacity.

In actual practice, such parallel conductivity is needed to allow for irregularities in the root temperature and for punctures in the radiator skins by micrometeorites and other debris. If there were no transverse conductivity, punctures in the skin would isolate the portions of the skin outboard of the hole from the heat pipe, removing that isolated area from the thermal transfer process. Conductivity parallel to the heat pipe allows thermal energy to flow around punctures.

Thermal conductivity in graphite-aluminum composites are highly anisotropic. In the fiber direction, conductivity can be very high; theoretical conductivities in excess of 1000 W/mK have been predicted for certain experimental high conductivity fibers in aluminum. For comparison, the conductivity of aluminum is about 200 W/mK and silver about 400 W/mK.

Perpendicular to the fibers, in either the in-plane or through-plane directions, conductivity can be lower by a factor of 10 or more, depending on fiber species and volume fraction.

In view of the orthotropic nature of the composite thermal conductivity, the first choice for orientation is to have the fibers perpendicular to the heat pipe, maximizing thermal conductivity away from the heat source. The reduced conductivity parallel to the heat pipe will have some as-yet undetermined effect on sensitivity to the radiator punctures in the skin. (Of course, punctures in the heat pipe itself would disable the entire radiator, not merely reduce its thermal transfer rate.)

The test matrix prepared at the beginning of the effort included many panels with low-angle cross plies, orienting fibers away from the direction perpendicular to the heat pipe. These panels, thermally less than optimal, were included under the assumption that structural considerations, especially the resonant frequency requirement, would be met only with composites containing off-axis fibers.

We determined that the vibration requirement could be met without the lengthwise stiffening of off-axis fibers. The multiplicity of cross-ply panels were eliminated from the contract during the modification with no loss of needed data. The final composite configuration designed for the radiator contained only fibers oriented perpendicular to the heat pipe, the thermally optimal configuration.

Six test panels were prepared for thermal conductivity and radiative transfer performance measurements. The test panels and measurements made are listed in Table 1.1. The various configurations are shown in Figure 8.

A total of 6 thermal conductivity measurements were made. Only one measurement was made on each of the two panels with isotropic properties (Cu and Al). Three measurements in orthogonal directions were made for the  $0^\circ$  unidirectional composite panel. For the two panels with rotational symmetry ( $45/45$  and  $0^\circ/90^\circ$  crossplies), only one in-plane measurement was taken. One thru-plane conductivity measurement was taken; the composite panels were indistinguishable in that direction. The panel listed as Tapered did not have a constant conduction area and was not suitable for measurement of thermal conductivity directly. Other than varying thickness, its configuration was identical to that of the  $0^\circ$  unidirectional panel.

All six panels were subjected to radiative thermal transfer testing. These tests were designed to determine the effect of composite configuration on the ability of a panel to transfer thermal energy away from a heat source along one edge, across the face of the panel to be radiated through vacuum to a liquid nitrogen-cooled cold plate. Seven radiative transport measurements were taken in total.

The methods and results of all measurements are contained in the following paragraphs.

### 1.3.1 Measurement Technique: Thermal conductivity.

Thermal conductivity in the two in-plane directions was measured using specimens approximately 25 cm (10 inches) long by 1.0 cm (0.5 inch) wide. The thickness of each specimen was equal to the thickness of the panel from which it came, nominally 1 mm.

A resistor was attached to one end of each using conductive epoxy. The heavy-wire leads to the resistor were cut short and electrical connections made through a pair 30 gauge wires. The smaller section wires were used to minimize heat loss from the resistor through the leads. A copper tube for water-cooling was attached to the opposite end with the same adhesive. A regulated voltage power supply was connected to the resistor and the a water source connected to the cooling tube. five thermocouples were attached to the specimen over a distance of 15 cm (6 inches) (Figure 9). The thermocouples were far enough from either the cooling tubes or the resistor to be free of end effects, assuring a uniform flux density throughout the area conducting section.

The specimen was well insulated by wrapping it in several layers of ceramic wool.

Power levels ranging from 0.1 watt to approximately 2 watts were supplied to the resistor. The voltage and current supplied to the resistor was measured with a digital voltmeter accurate to .01 volt



Table 1.1

## Radiative Transfer Test Panels

Panel	Size	Tests Conducted				
		Thermal Conductivity			Thermal Transfer	
		X	Y	Z	X	Y
Copper	10X10X.050	X			X	
Aluminum	10X10X.063	X			X	
Graphite-Aluminum	10X10X.029	X		X	X	X
0°						
0/90	10X10X.032	X			X	
±45	10X10X.030	X			X	
tapered	10X10X (.025-.008)				X	

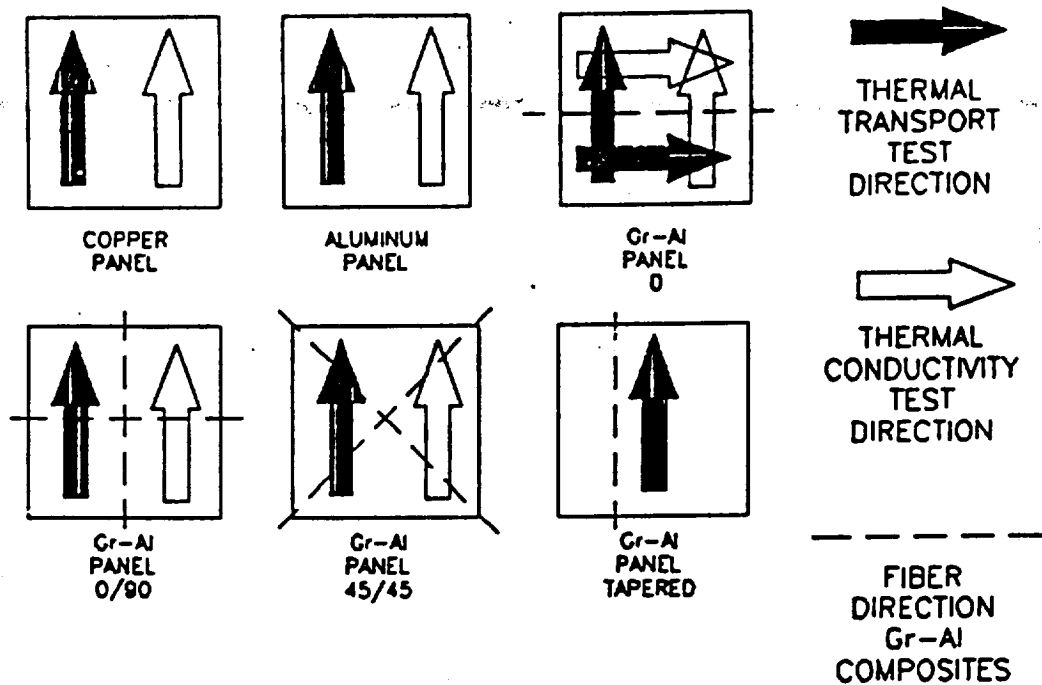


FIGURE 8  
Radiative Transfer Test Panels

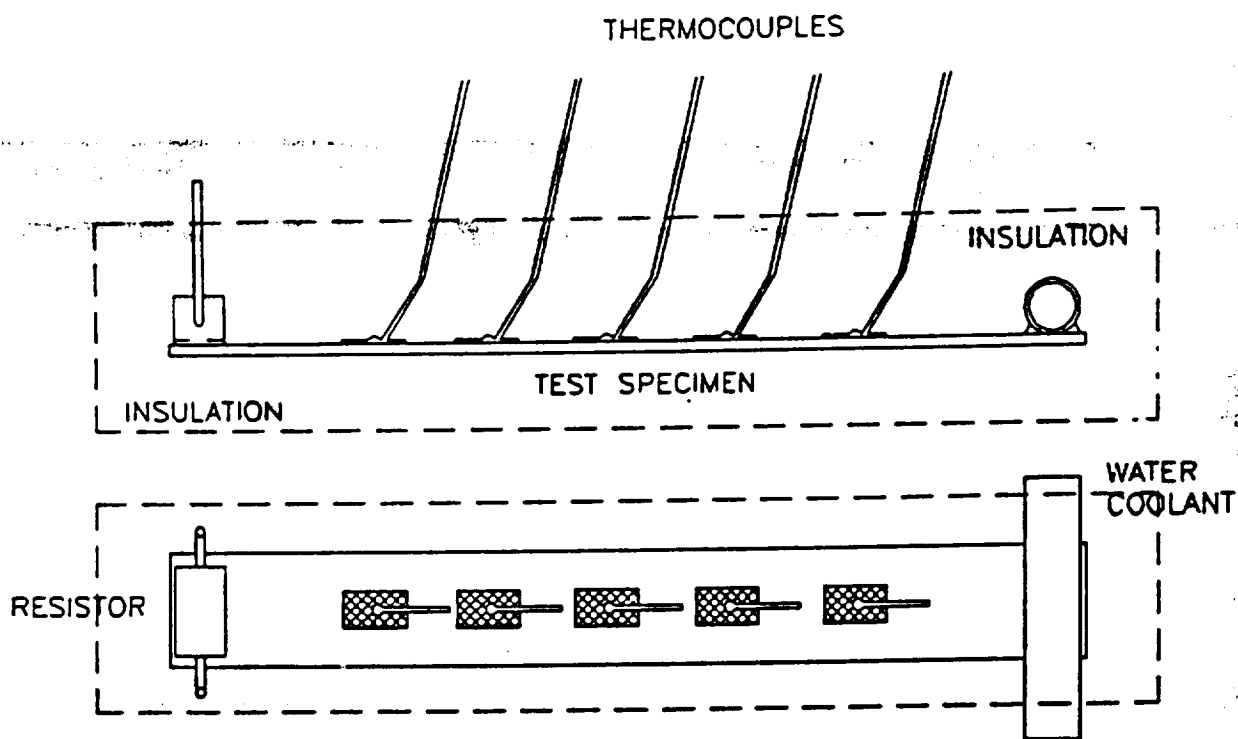


FIGURE 9  
In-Plane Thermal Conductivity Measurement

and .001 amp, respectively. The temperature at each thermocouple was measured to  $0.1^{\circ}\text{C}$  and their spacing measured to 0.5 mm. After the specimen had reached equilibrium at a given power input level (typically 15 minutes), the temperatures at the thermocouples measured.

The thermal gradient across the specimen was calculated using a least-squares best fit. Using the temperature gradient along the specimen, the geometry of the specimen and the power input, the thermal conductivity was determined using the formula

$$k = q A^{-1} (dT/dx)^{-1}$$

where  $k$  is the thermal conductivity in  $\text{W/mK}$

$q$  is the power flux through the specimen in watts

$A$  is the cross sectional area of the conduction path  
and  $dT/dx$  is the thermal gradient in  $^{\circ}\text{C/m}$ .

An error propagation analysis shows the expected standard deviation in the reported thermal conductivity to be about 4% or  $\pm 12 \text{ W/mK}$  at  $300 \text{ W/mK}$ .

Through-plane thermal conductivity was measured in the fixture shown in Figure 10. Ten 2.5 cm square coupons from a single specimen panel were bonded into a stack approximately 1.5 cm thick using high conductivity silver-filled epoxy. The stack was heated from one side by an electrical heater coupled to the specimen by a copper block. The opposite side was contacted by a similar copper block cooled by running water. The temperature of either face of the specimen was measured at the faces of the copper cooling and heating blocks. Temperatures at one additional point in the heating and cooling blocks were measured as well. The power input was calculated by measuring the temperature gradient through the copper blocks after the test set had reached thermal equilibrium. The conductivity through the specimen was calculated from the temperature gradient across the specimen stack, the power input and specimen geometry using the same formula as above. An error analysis shows approximately 4% uncertainty in the thermal conductivity determination.

### 1.3.2 Results of thermal conductivity measurements

The results of the thermal conductivity measurements are presented in Table 1.2.

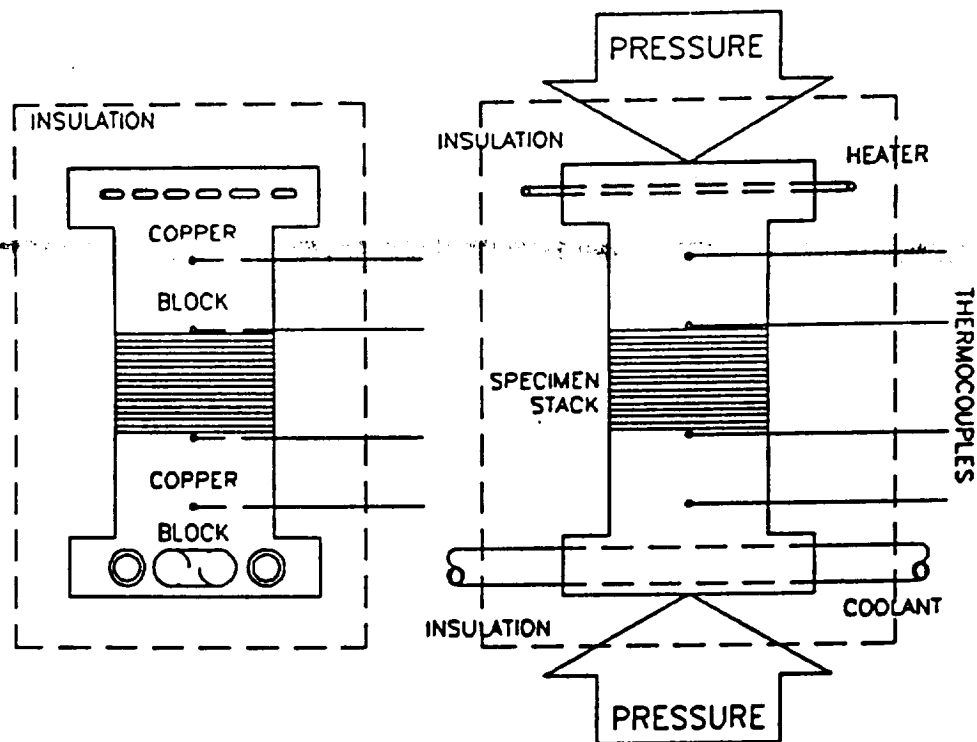


FIGURE 10  
Thru-Plane Thermal Conductivity Measurement

**Table 2.2**

**Thermal Conductivity Measurements**

Panel	Thermal Conductivity $\left[\frac{W}{mK}\right]$		
	X	Y	Z
Copper	360	-	-
Aluminum	190	-	-
Graphite-Aluminum			
0°	310	60	40
0/90	185	-	-
±45	140	-	-
tapered	-	-	-

### 1.3.3 Measurement Technique: Radiative Transfer

The radiative transfer testing was carried out in a thermovacuum chamber constructed by DWA. The chamber enclosed a volume 45cm by 45cm and 22cm deep. A 40cm by 40cm liquid nitrogen-cooled cold plate was mounted on one interior surface and equipped with feed throughs for the flow of coolant. Additional feed throughs were provided for 14 sets of thermocouple leads and one set of power leads. The chamber is shown in Figures 11 through 13.

All the panels being tested were 25cm square and approximately 1.5mm thick. The panels are listed in Table 1.1. With the exception of the copper panel, all the panels were subjected to a surface conversion process to control their optical properties. The process had been developed for NASA by Boundary Technology, Inc., of Buffalo Grove, IL. Details of the process were provided to local vendors used by DWA during this program.

The process consisted of an acidic bright dip to increase the reflectivity of the aluminum surfaces followed by an anodization to increase the emissivity at the long wave lengths being radiated. The result was a surface with an emissivity in excess of 0.7 and an absorptivity less than 0.2. The surfaces of the copper panel were cleaned, but otherwise left as fabricated.

Twelve Type K thermocouples were attached to each panel tested as shown in Figure 14. The thermocouples were mounted on high temperature polymer tape and pressed against the surface to be monitored. Additional thermocouples were mounted on the cold plate and the chamber wall. The thermocouples were connected to a computer-controlled data acquisition system and monitored automatically.

Each panel to be tested was equipped with a silicon rubber strip heater strip clamped along one edge. Energy was applied to the heater by a power supply. The voltage and current were measured by a digital voltmeter. The temperature of the heated edge was measured on the side of the panel opposite the heater.

The cold wall was cooled by a flow of liquid nitrogen through channels machined into the plate. The LN2 was supplied by a 22-liter canister pressurized to approximately 17 psi. The flow of nitrogen was controlled by two valves: a supply valve at the canister and a throttle valve at the outlet port of the cold wall. Escaping nitrogen was vented directly into the air. To cool the wall, both valves were opened and nitrogen allowed to flow freely until the cold wall was at a sufficiently low temperature. The temperature was maintained within 2°C by adjusting the throttle valve during the test.

To measure the thermal transfer of a panel, the power to the heater strip and the temperature of the cold wall adjusted to meet the test conditions when the panel had reached thermal equilibrium. When the temperatures being monitored by the data acquisition system stopped changing, the voltage and current being supplied to the heater were measured and the power input calculated. The temperatures of the heater on panel and the cold wall were the same in each test. The power being transferred was then directly compared for each panel configuration.

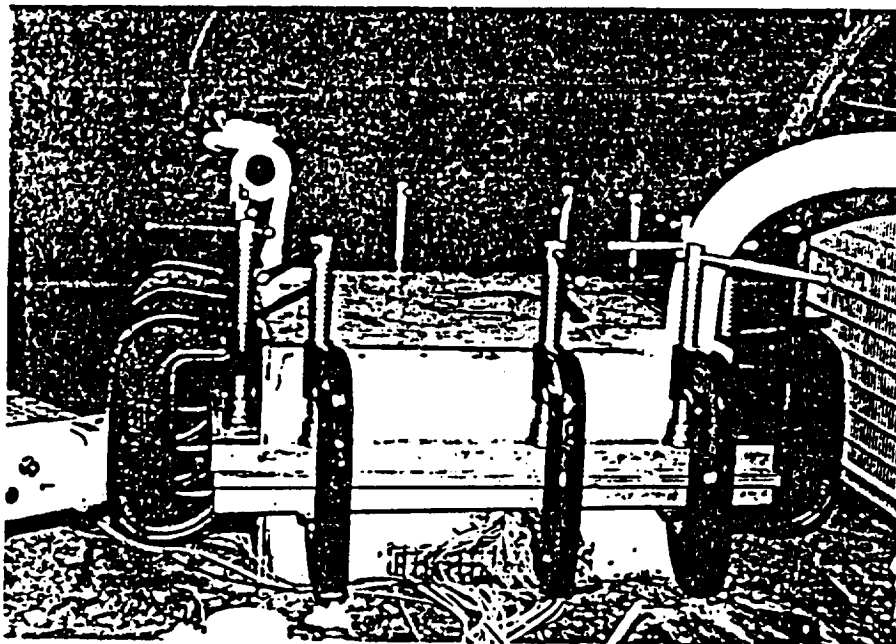


FIGURE 11  
Thermovacuum Chamber



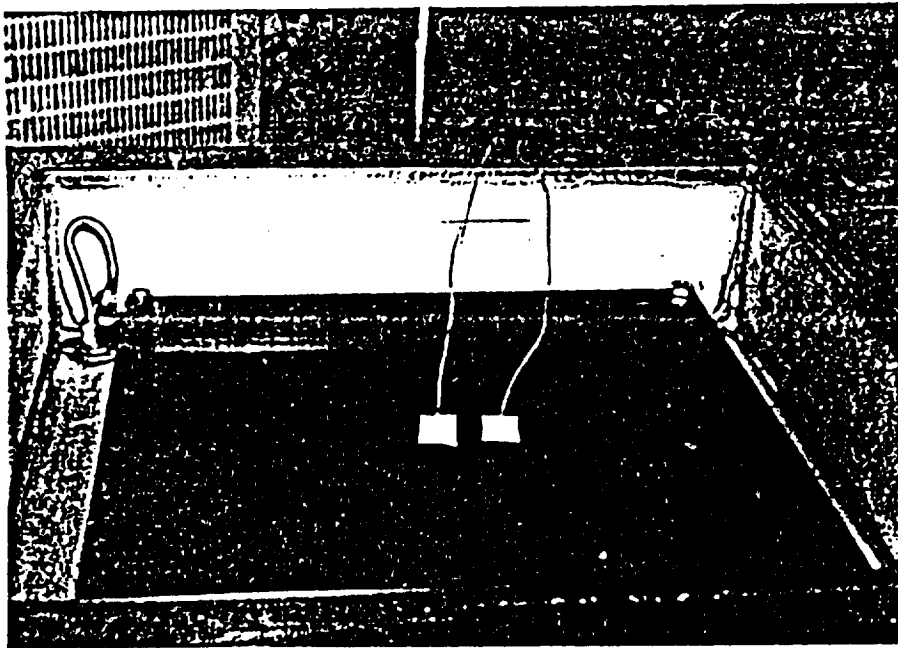


FIGURE 12  
Thermovacuum Chamber

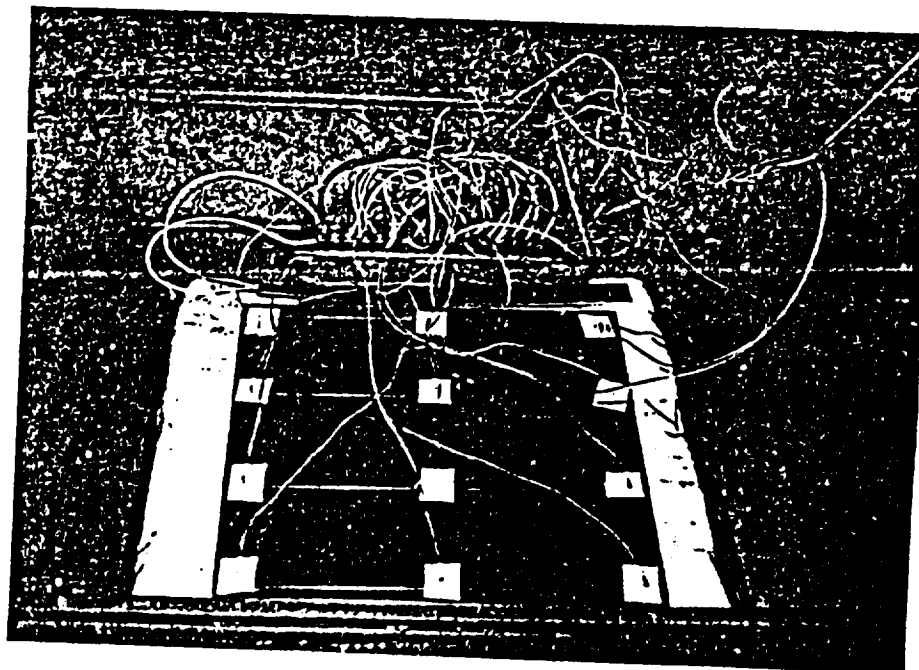
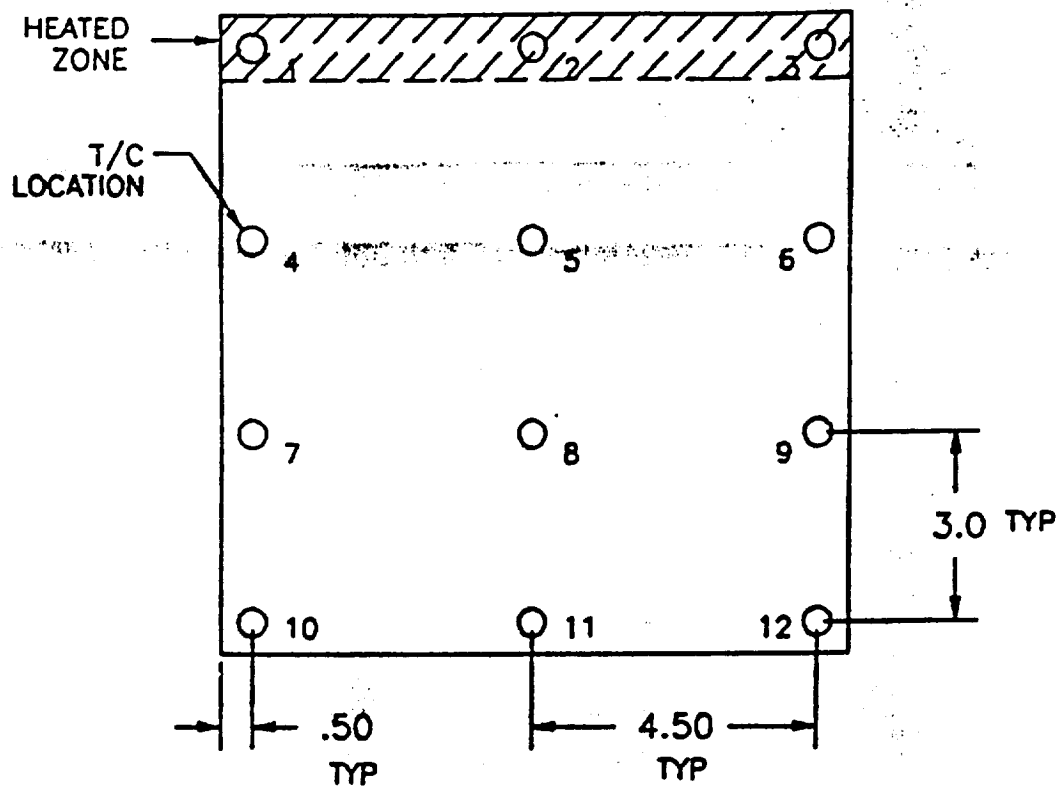


FIGURE 13  
Thermovacuum Chamber



(Dimensions are in inches)

FIGURE 14  
Thermocouple Layout  
Radiative Transfer Tests

### 1.3.4 Results of Thermal Transfer Testing

The results of the thermal transfer tests are shown in Table 1.3

### 1.4 Off-gassing by Graphite-Aluminum Under Vacuum

The mass lost by off-gassing under vacuum was determined by weighing a sample before and after a one-week exposure to vacuum. The panels used in the thermal transfer testing were too large to fit into the most accurate analytical balance available ; a smaller sample was taken for test.

A sample having an approximate mass of 46 grams was thoroughly cleaned with soap and water followed by acetone, dried and baked out under heat lamps at a temperature of 260°F for one hour. After cooling to room temperature, the sample was weighed to a precision of 100 micrograms. To determine the accuracy of the electronic scale, the sample was weighed 10 times, re-zeroing the balance after each weighing. The reported weight is the mean value and standard deviation of the ten independent weighings.

The sample was then enclosed in the vacuum chamber and held at a vacuum of  $10^{-4}$  torr for one week, removed and reweighed in the same manner.

There was a measured loss of mass of  $.0009 \pm .00032$  grams or .002%.

Initial mass :  $(45.911 \pm .00023)$  gm

Final mass :  $(45.9202 \pm .00023)$  gm

Mass loss :  $(0.0009 \pm .00032)$  gm

We feel the result of this measurement confirms our statement that there is no off-gassing by graphite-aluminum under vacuum.

### 1.5 Radiator Panel Configuration

The primary driver for the design and construction of this radiator was to investigate the ability of high thermal conductivity graphite-aluminum composite materials to reduce the weight of a

Table 1.3

Radiative Transfer Test Results

Panel	Mass (gm)	Power Input (W)	Panel Temperatures				Sink Temp (K)
			T2	T5 (K)	T8	T11	
Copper	660	3.9	286	283	283	283	116
Aluminum	273	13.3	284	F	F	F	106
Graphite- Aluminum							
0° (Long)	115	11.7	285	F	F	F	103
(Trans)	115	6.7	283	283	F	281	102
0/90	115	8.8	295	F	F	F	91
±45	111	10.9	284	271	263	259	102
tapered	57	10.6	284	269	257	251	102

Note: (F) indicates loss of data during test

radiator without loss of thermal transfer capacity. In keeping with that objective, an analysis of the optimal profile for a radiating panel was performed by Dr. Eugene Ungar of NASA JSC. His analysis produced a design for a tapered section radiator panel. The profile of the taper was such that the thermal flux density was constant throughout the conductivity path and the temperature profile linear from the root of the radiating panel to the outer edge (Figures 15 and 16). Dr. Ungar calculated the tapered design would result in a 30% reduction in the weight of the radiating panels with no significant reduction in thermal transfer.

The radiating panels were to be fabricated by stacking and diffusion bonding layers of graphite-aluminum of varying widths, approximating the specified profile

The ideal design called for a smooth taper in panel thickness from .6 mm (0.025 inch) at the root to 0.13 mm (0.005 inch) at the outer edge. The manufacturing process by which DWA produced the graphite-aluminum composite for the radiator panels results in a nominal ply thickness of 0.13 mm. As a result, the profile was approximated by a series of five steps of 0.13 mm each (Figure 17).

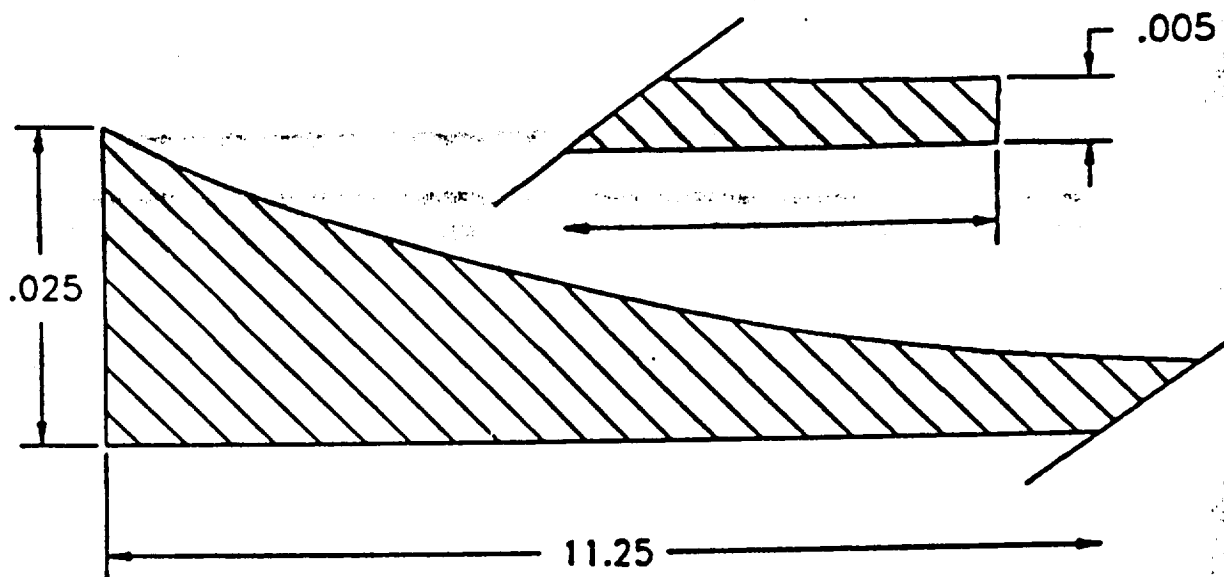
In order to achieve the best thermal conductivity away from the heat pipe, the composite radiating panels were designed to incorporate 50% (by volume) unidirectional high conductivity 120Msi graphite fibers, all oriented perpendicular to the heat pipe. The thermal conductivity of the fibers in the longitudinal direction was approximately 520 W/mK (manufacturers data). The thermal conductivity of the composite was expected to be about 360 w/mK.

The basic panel size was to be .6 meter by 1.5 meter, with two panels constituting one radiating set around the heat pipe (Figure 18).

During manufacturing trials investigating the attachment of composite panels to the round heat pipe, it became apparent that the original panel design was too stiff to conform to the pipe as desired. To facilitate this attachment, the basic panel size was reduced to .3 m by 1.5 m and a 2 cm region along the edge of the panel where it attached to the heat pipe modified to improve its to the circular heat pipe section. This was accomplished by replacing four of the five ply thickness with unreinforced aluminum at the edge. The final panel configuration is shown in Figure 19. Finite-element thermal analysis of the radiative transfer characteristics of the panel showed no significant change resulting from the modification.

## **1.6 Radiator Structure**

The lenticular section (Figure 20) incorporated in the radiator design accomplished two goals: it satisfied the 1.5 mm edge radius requirement and it provided protection for the vulnerable thin edge of the tapered panels.



(Dimensions are in inches)

FIGURE 15  
Tapered Radiator Thickness Profile

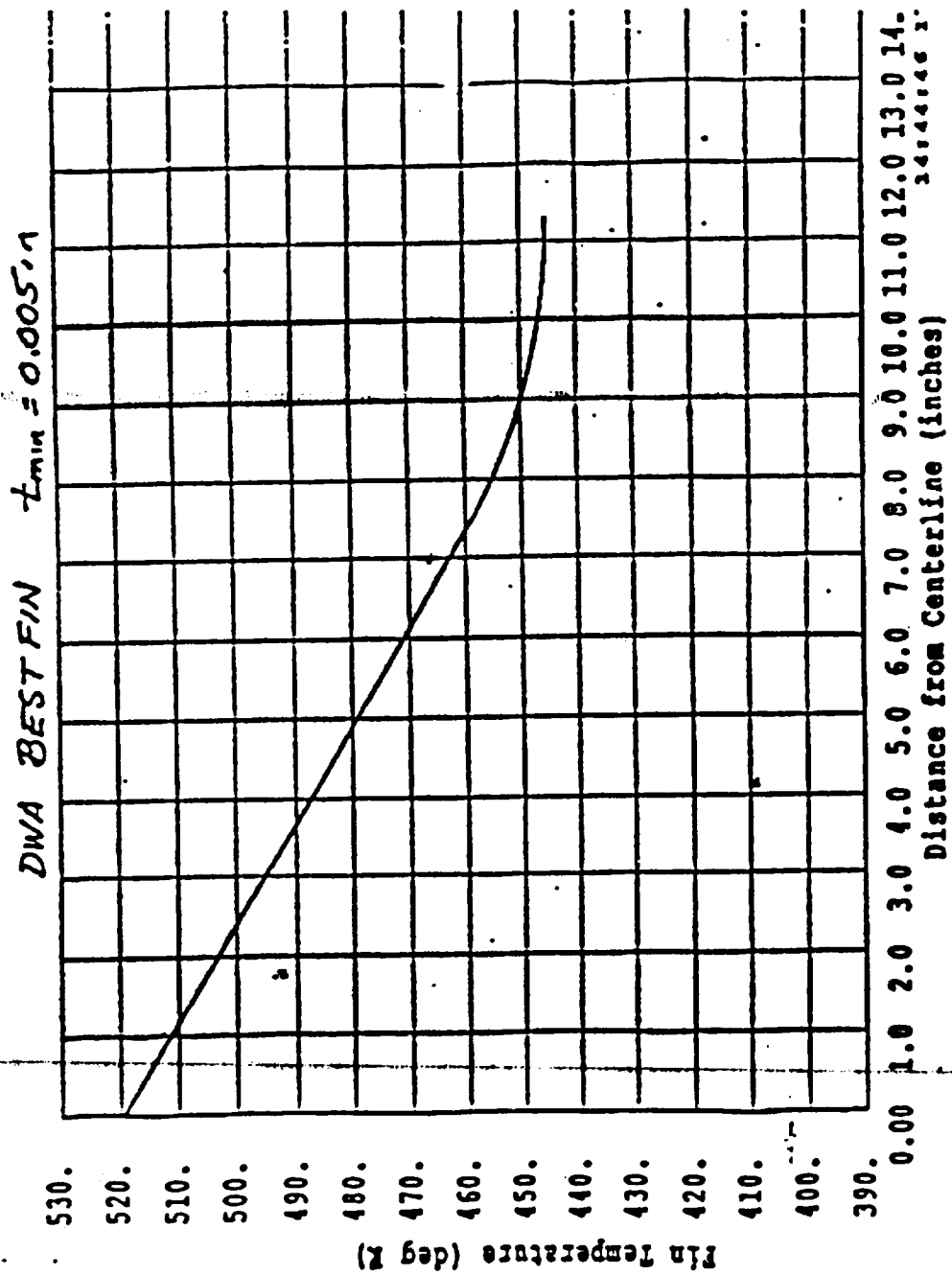


FIGURE 16  
Tapered Radiator Temperature Profile



DIMENSIONS  
ARE IN  
INCHES

50% P100/  
6061 with  
1100 Al  
facesheets

.005  
TYP

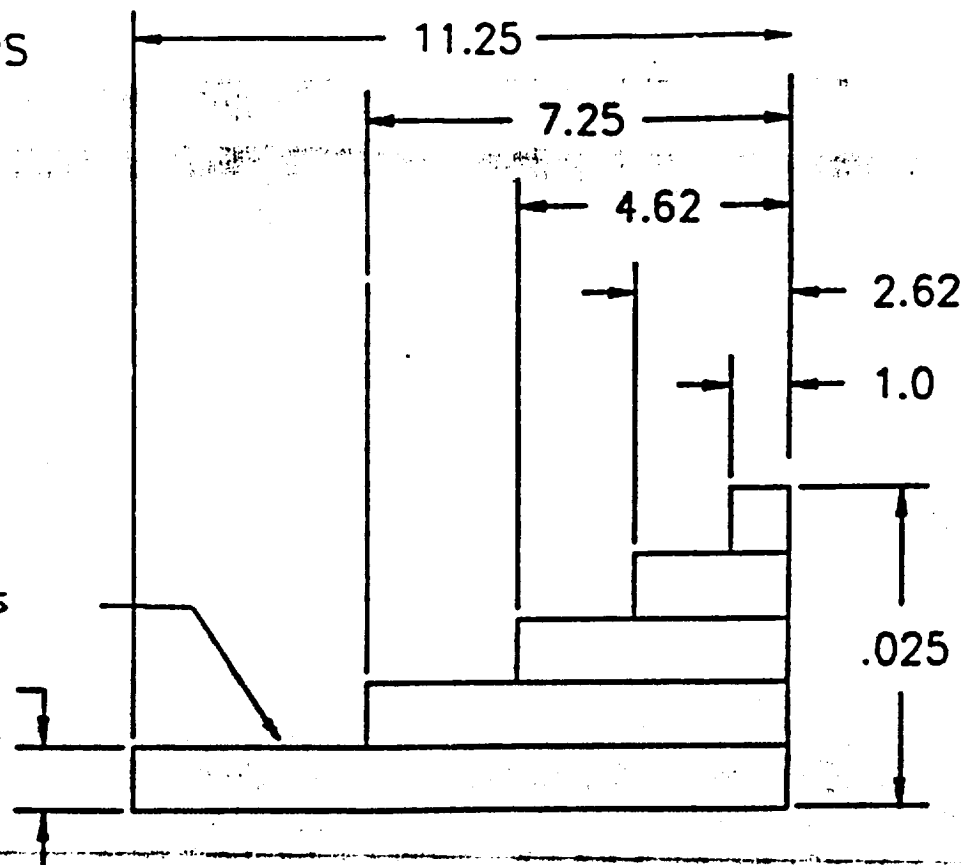


FIGURE 17  
Stepped Radiator Thickness Profile

RADIATOR

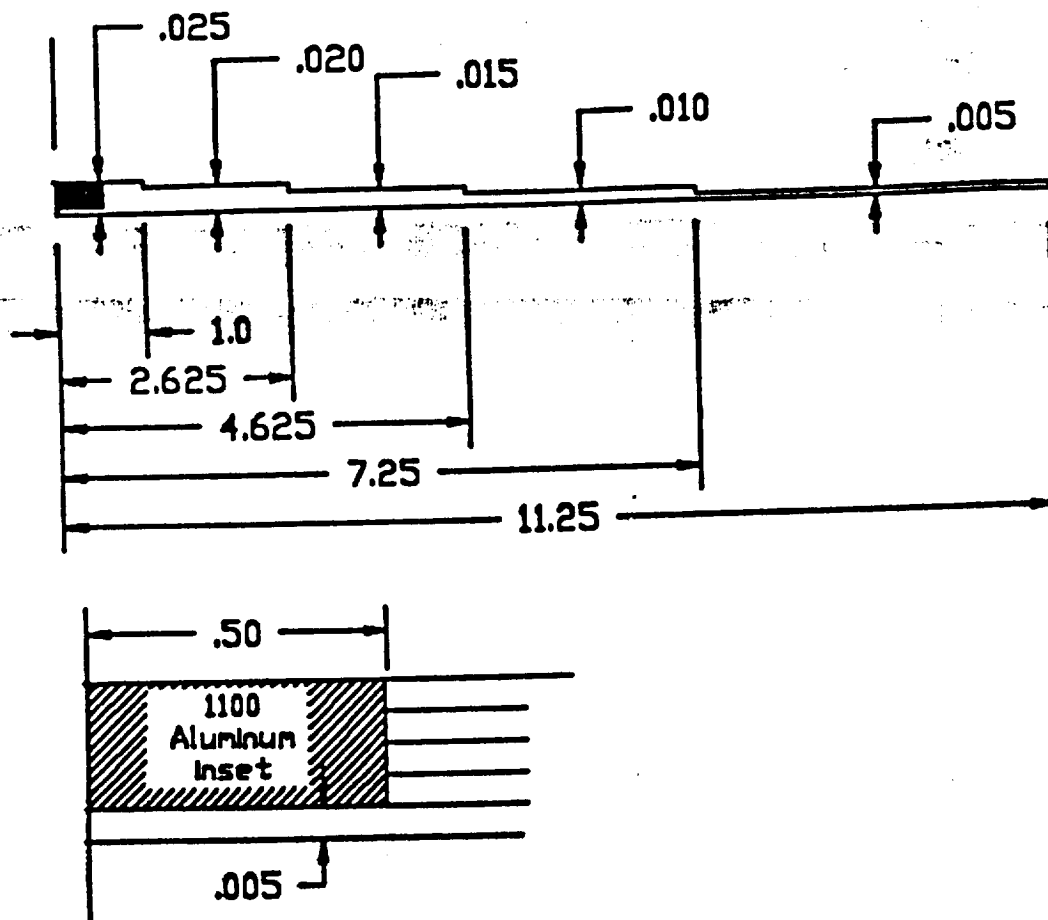
1 2

1.5m

HEAT PIPE

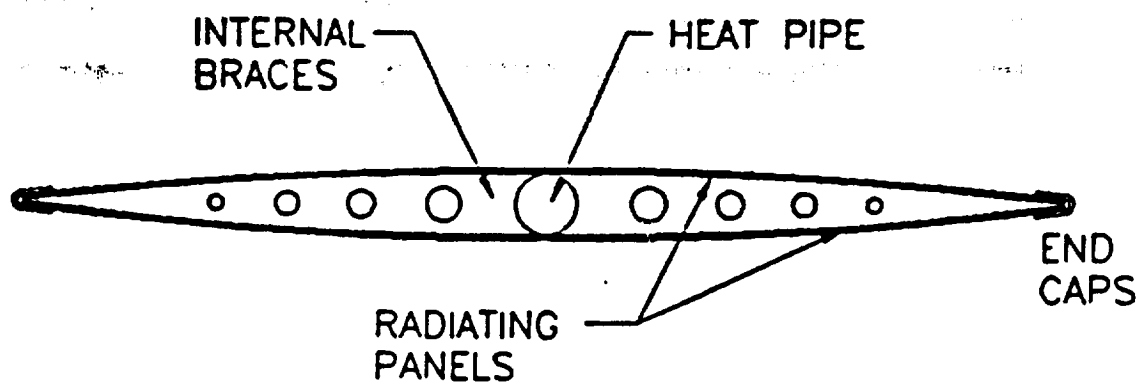
0.6m

FIGURE 18  
Radiator Panels Around Heat Pipe



(dimensions are in inches)

FIGURE 19  
Stepped Radiator with Aluminum-rich Zone



**FIGURE 20**  
**Lenticular Section Radiator**

The components in the radiator assembly were

- a, Thermocore folding heat pipe (Figure 21) (1) each
- b, DWA tapered Gr-Al panels (36) each
- c, radiator braces (Figure 22) (60) each
- d, radiator panel edge caps (Figure 23) (18) each.

The radiating panels were formed at the aluminum rich edge to match the curvature of the heat pipe. Forming was required to maximize the area of contact between the radiator and the heat pipe, reducing the thermal resistance at the junction. The attachment was made with a high conductivity filled epoxy (Appendix 2).

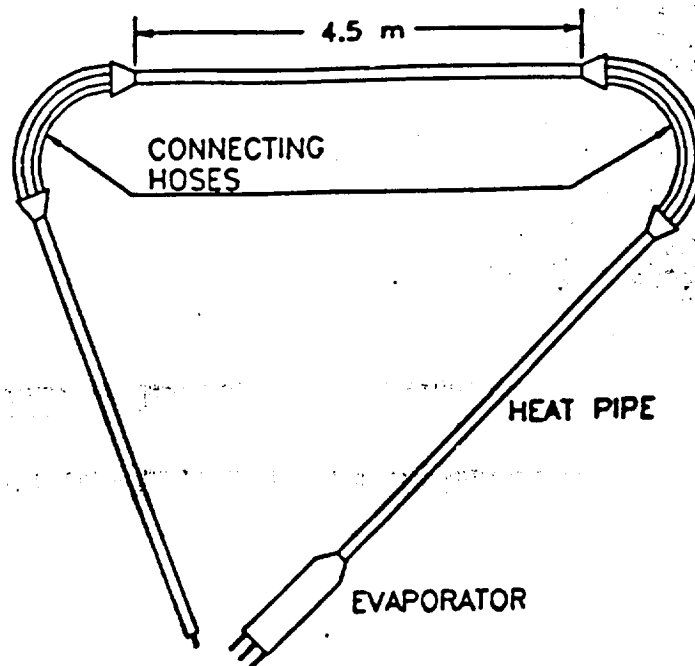
The spacing of the radiator braces (Figure 24) was chosen to provide the minimum required support for the radiating panels and to add minimum weight to the structure. The spacing is set to support each panel at the ends and at third points across its span. The braces were designed to nest inside the formed edge cap and provide a continuous surface for the attachment of radiating panels (Figure 25). Holes were provided in the brace for weight-reduction and to open the closed chambers created in the structure. Edge caps were spliced with small aluminum inserts between braces (Figure 26). All joints were made with a structural adhesive (Appendix 3).

The radiator assembly does not meet the resonant frequency requirement. Most of the structural stiffness in the designs analyzed in the initial stages of this effort came from the heat pipe shown in Figure 5. The experimental heat pipe used in the construction of the radiator has very low stiffness, being primarily an aluminum tube with sintered aluminum in the interior. The resonant frequency of a continuous 15-meter lenticular radiator of the design described above would be approximately .13 hz. It was decided that the thermal transfer characteristics would be of overriding importance in this radiator, constructed as it is with a folding heat pipe.

## 2.0 RADIATOR FABRICATION

The radiator construction followed the following sequence:

- 1, fabricate graphite-aluminum panels
- 2, fabricate assembly jigs and fixtures,



430FINAL:430FIG5.DWG

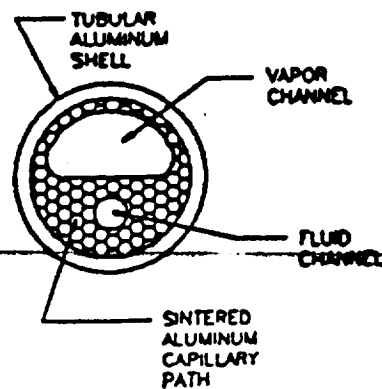
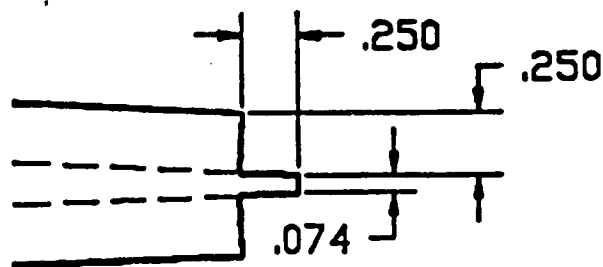
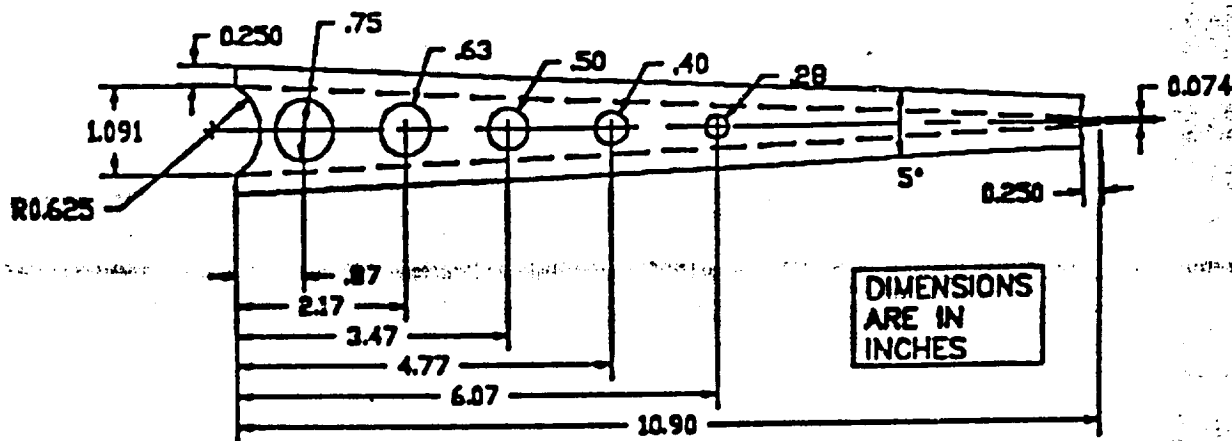
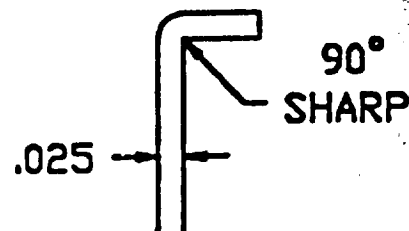


FIGURE 21  
Folding Thermocore Heat Pipe



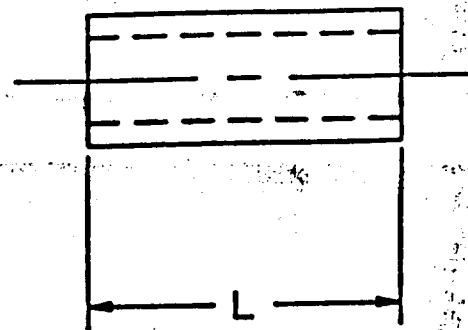
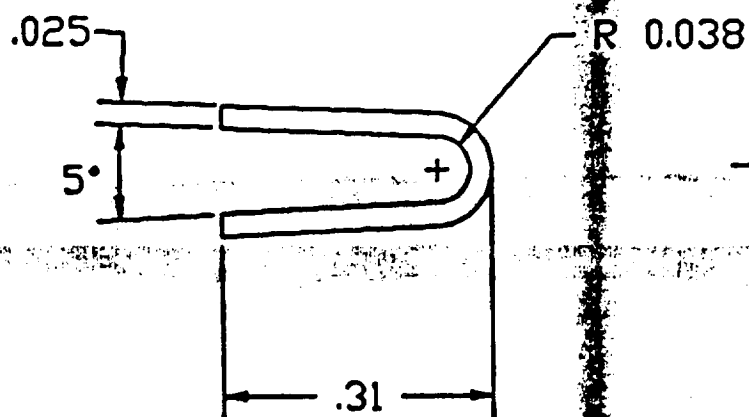
TIP DETAIL



TYPICAL BEND

MAT'L: 3003-H14 AL  
REQ'D: 60 PIECES

4307NAL:43071023.DWG

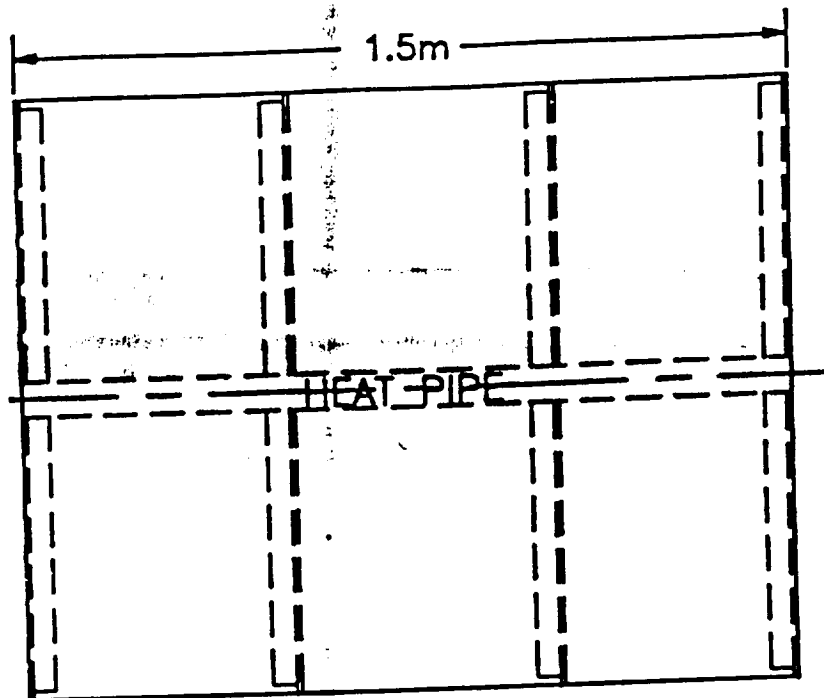


L: (18) pcs @ 59.5  
 Mat'l: 6061-T6 Al

DIMENSIONS  
 ARE IN  
 INCHES

430FINAL-430PG24.DWG





430FINAL-430FIG25.DWG

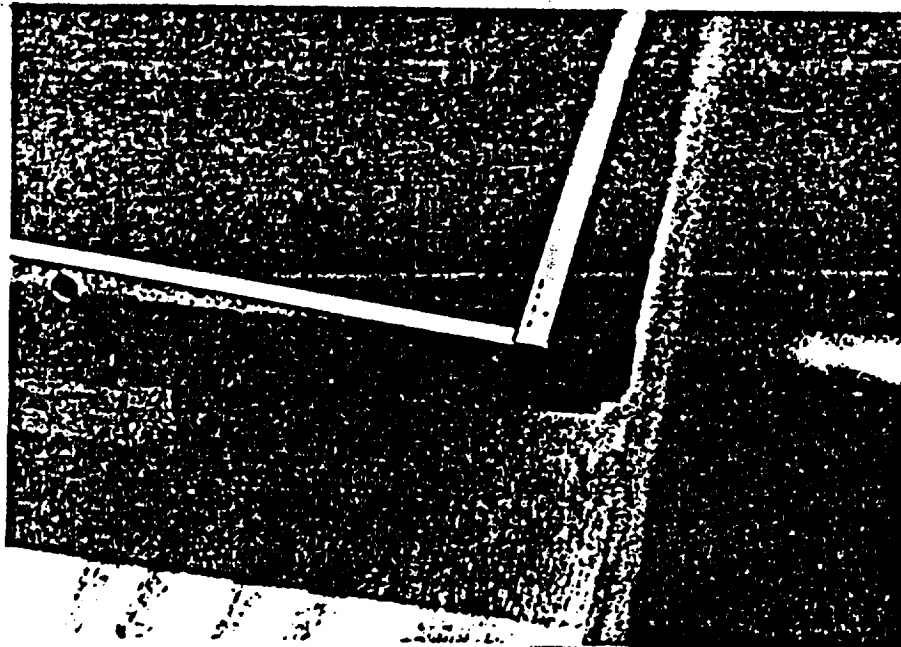


FIGURE 25  
Edge-Cap to Brace Attachment

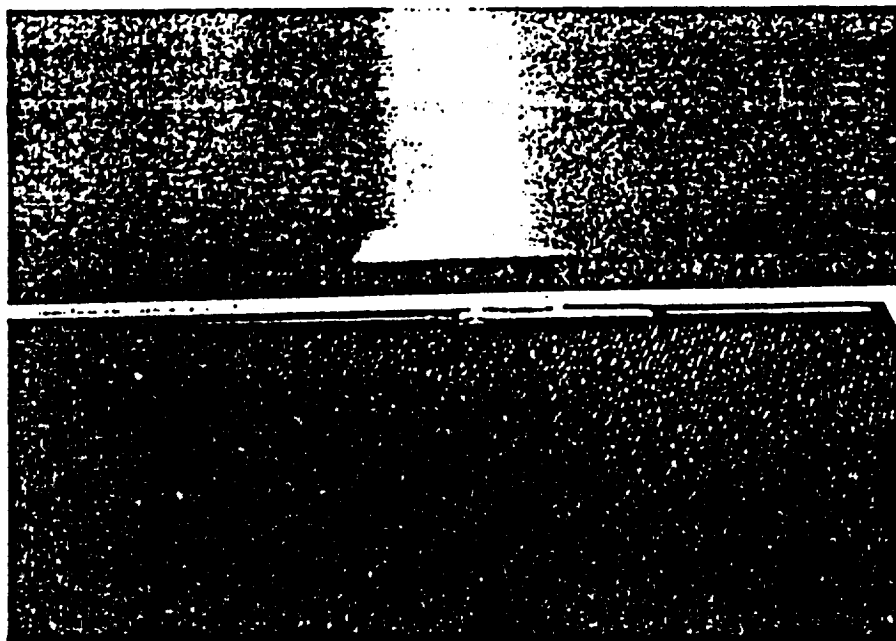


FIGURE 26  
Edge-Cap Splice

- 3, fabricate braces and end caps,
- 4, attach braces and end caps to heat pipe,
- 5, attach graphite-aluminum panels to radiator structure.

## 2.1 Fabricate graphite-aluminum panels

Thirty-six graphite aluminum panels were needed for the construction of the radiator. The details of the manufacturing technique are proprietary and will not be discussed. Each panel was fabricated of high modulus (120Msi) graphite with an approximate thermal conductivity of 520 W/mK. The fibers were unidirectional and comprised 50% of the composite, balance being either 1100 or 6061 aluminum alloy. The calculated thermal conductivity of the composite was 360 W/mK in the fiber direction.

The initial manufacturing trials were done on panels 0.6 meters by 1.5 meters, with all graphite fibers running in the 0.6 m direction. The panels were symmetrically tapered from 0.64 mm thick down the center (.3 meters from either long edge) to 0.13 mm at both edges. There was no aluminum rich region at the center.

The initial plan for the fabrication of the radiating panels called for the surfaces to be subjected to the experimental anodizing conversion process described in Section 1.1.3. After trials with small test coupons and one full sized tapered panel, it was decided to eliminate that step from the process, although it had been successful in each of the trials conducted.

The decision was made based on the uncertain reliability of the process applied to large panels. The panels made for this radiator are costly and there were only a small number of spare panels for replacing any damaged during assembly or processing. Although the anodizing process worked well with the small coupons processed in a laboratory environment, it was felt the transition to full scale production in a commercial facility was somewhat hazardous, with an unknown probability of damage to the panels during processing. Because NASA had available more conventional surface preparations to control the absorptivity and emissivity and because the process was not specifically called out in the contract, it was decided by mutual agreement between NASA and DWA to leave the radiating surfaces bare. To protect the aluminum surfaces, a coating of clear acrylic was applied.

In preparation for the construction of the radiator, a representative section 30 cm long was fabricated to identify problems in assembly. The initial attempts were to attach full width 0.6 m sections of composite panel to the round heat pipe, forming the composite to the circular cross section and joining the outer edges into the lenticular section required (Figure 27). The extreme stiffness of the composite, bending the fibers to accommodate the curved surface of the heat pipe, rendered this approach impossible. No more than a line of contact was achieved at the point of tangency between the panel and the heat pipe and the forces needed to deflect and hold the panels in the required configuration was excessive. Maintaining the shape would have required braces be spaced very close

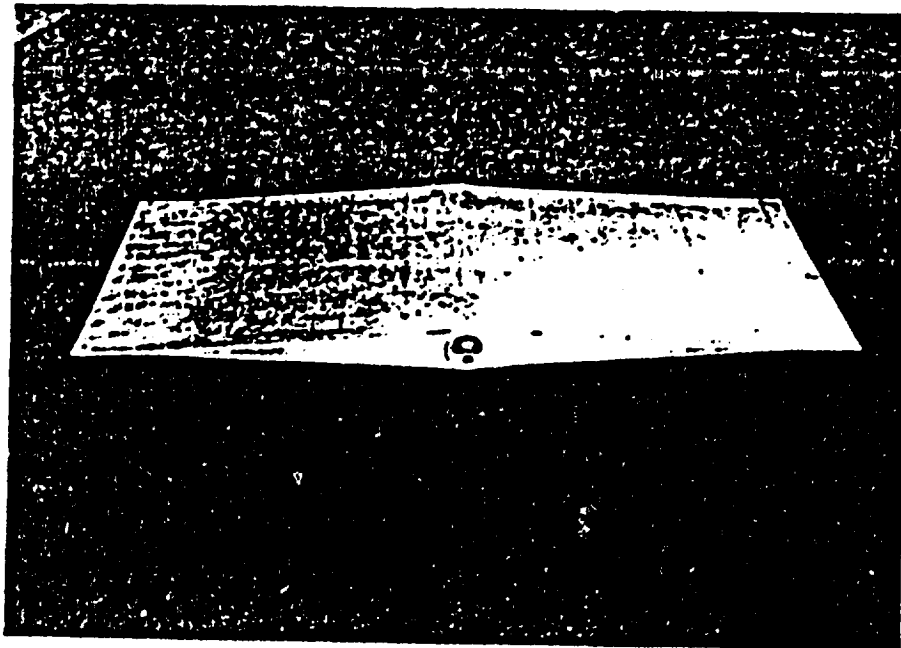


FIGURE 27  
Trial Lenticular Radiator Section

together (as many as one every 6 cm), negating any weight savings gained from the use of composite.

The model section was built by sanding the central 2 cm of each panel to a thickness of one graphite ply before attaching to the heat pipe (Figure 28). The sanding imparted a round section to the panel, more closely matching that of the heat pipe, and the thinness reduced the force needed to hold the panels in shape.

As a result of the experience gained in the construction of the model, it was decided to adjust the panel configuration, adding the aluminum rich section where the panel is to be formed to the heat pipe and reducing the width of the panels from a 0.6 meter symmetrical double taper to a 0.3 meter single taper. The panels would be joined by a seam along the heat pipe (Figure 29). Because there are no structural loads in that direction and no thermal transfer across that line, the division could be made with no loss of performance.

The panels were made in lengths of 1.5 meters. The length was chosen based on constraints of tooling capability for fabrication and anticipated length of folding heat pipe needed to equip with radiating panels. 1.5 meters is one third of the 4.5 meter length of each section of the heat pipe. It was planned to attach 12 panels to each of the three sections (Figure 30).

A total of 38 single-taper panels were fabricated for attachment to the heat pipe structure, providing 2 spares.

There was some waviness to some of the panels (Figure 31). At this point it is uncertain as to whether this waviness was the result of the tapered section or the presence of the aluminum-rich strip at the edge. The waviness affected the assembly procedures used, as described in Section 2.5.

## **2.2 Fabricate Braces and End-caps**

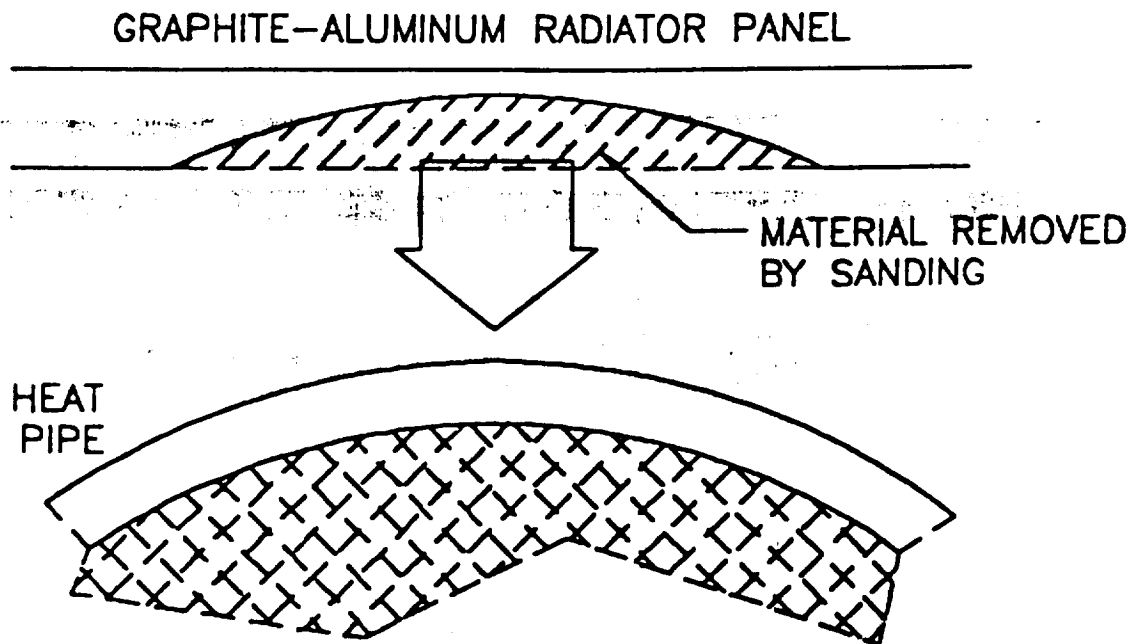
The radiator frame consisted of the heat pipe, internal braces and end-caps.

The internal braces are shown in Figure 32, fabricated at a local sheet metal fabricator in accordance with drawings provided by DWA. The braces were punched and formed of 3003-H13 aluminum alloy sheet 0.63 mm thick. Sixty braces are required for the radiator, 66 were made.

The end caps are shown in Figure 33. They were designed to fit over the outboard ends of the internal braces, joining them and completing the frame. The end caps were made by the same vendor fabricating the braces. They were made of 1100 aluminum alloy to achieve the radius of curvature needed.

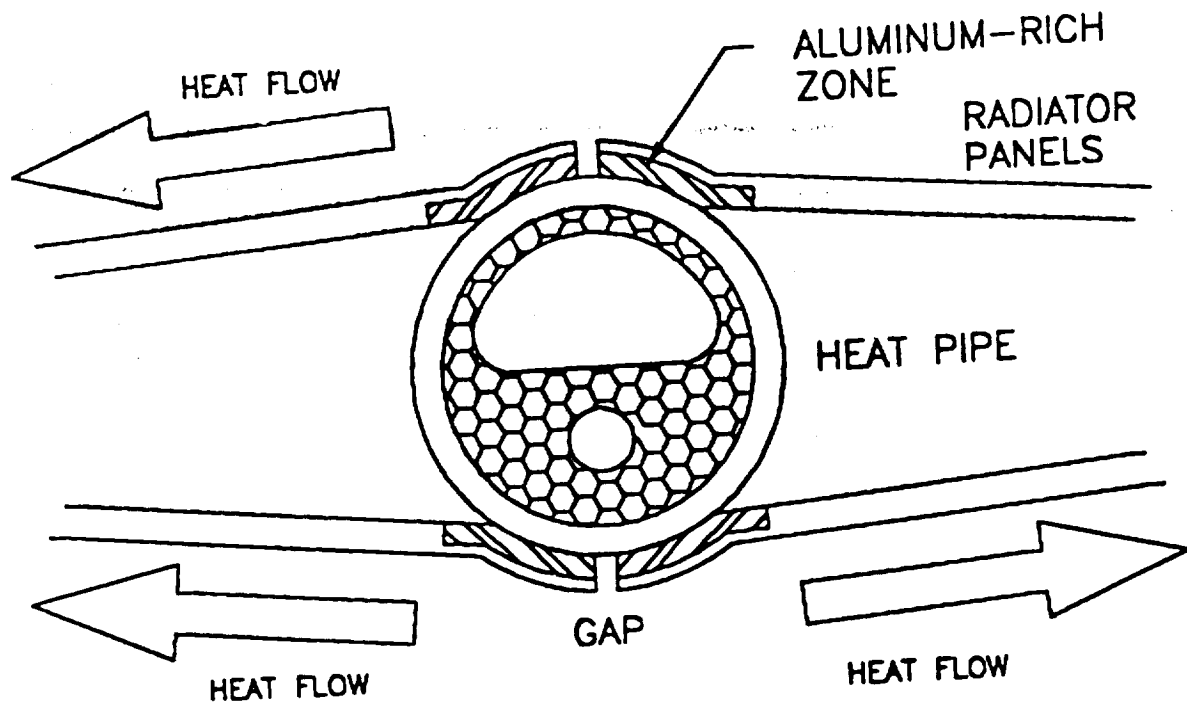
## **2.3 Fabrication of Assembly Jigs and Fixtures**

Four fixtures were constructed for assembly of the radiator: a cradle for holding the heat pipe and



430FINAL:430FIG30

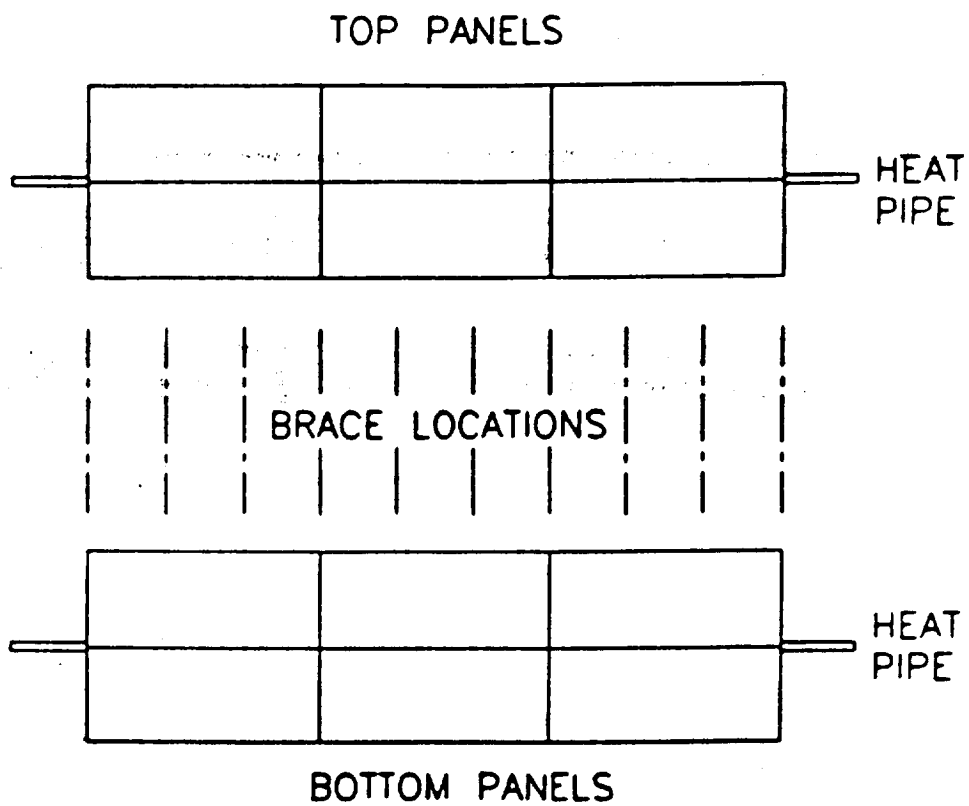
FIGURE 28  
Sanded Graphite-Aluminum Panel



430FINAL:430FIG31.DWG

FIGURE 29  
Seam in Graphite-Aluminum Panel at Heat Pipe





430FINAL:430FIG32.DWG

FIGURE 30  
Layout of Radiating Panels

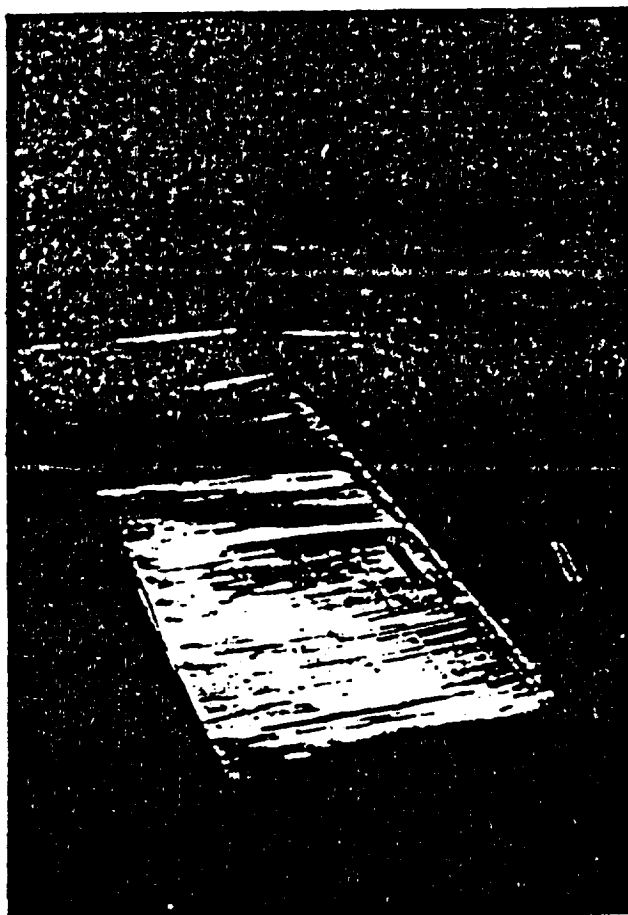


FIGURE 31  
Waviness in Gr-Al Panels

ORIGINAL PAGE IS  
OF POOR QUALITY

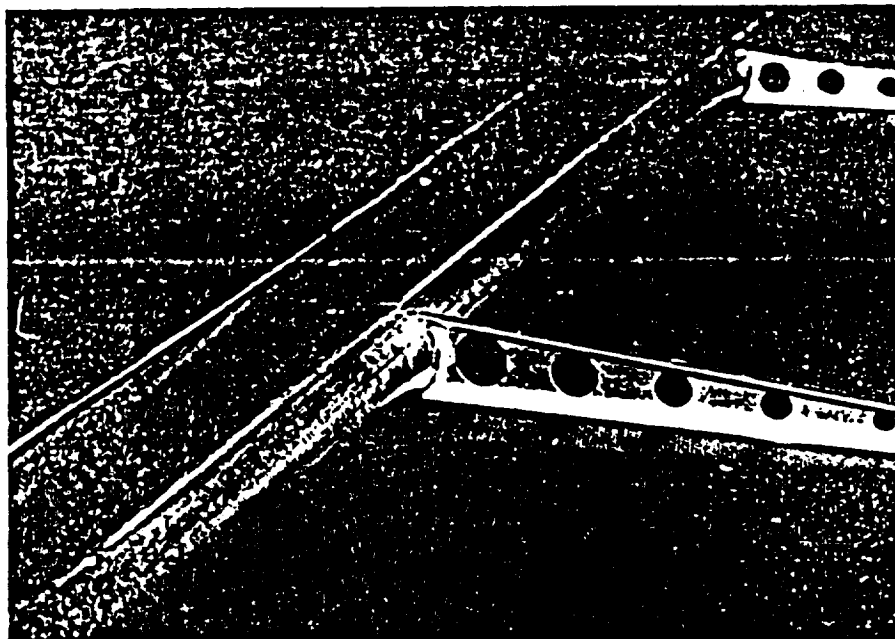


FIGURE 32  
Radiator Braces

ORIGINAL PAGE IS  
OF POOR QUALITY

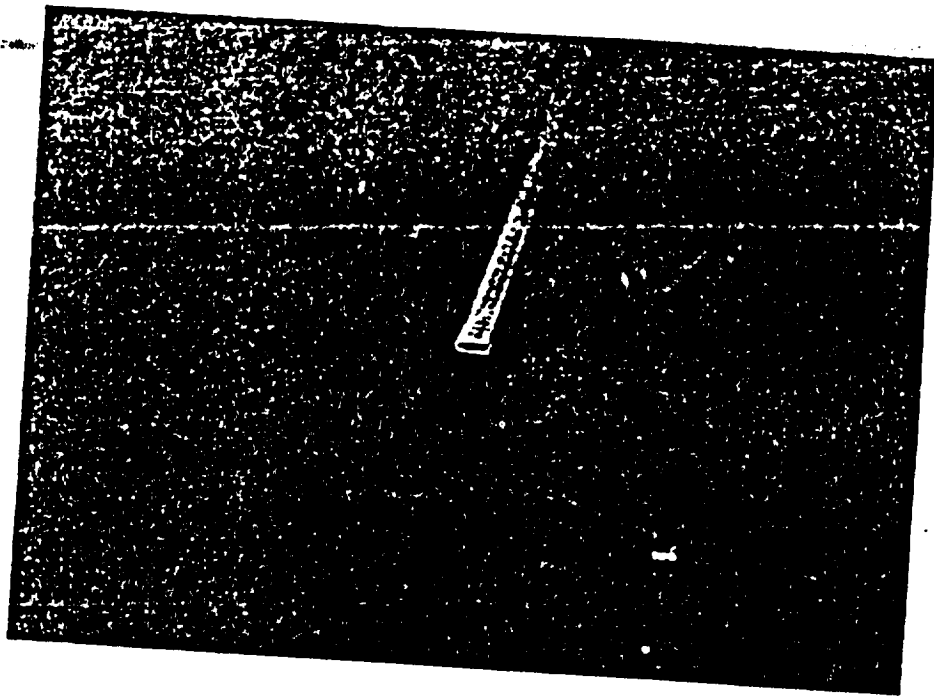


FIGURE 33  
Radiator Edge-Cap

braces in position for assembly of the radiator frame, a formed table to hold the radiator frame for attachment of the surface panels, padded pressure plates for pressing the surface panels to the frame during adhesive bonding and curing and a tool for creating the curvature in the attachment point of the panels matching that of the heat pipe.

### **2.3.1 Radiator Frame Cradle**

The frame cradle held the heat pipe and internal braces in position for assembly of the frame. One cradle was provided for each section of the folding heat pipe. Each cradle consisted of 20 wooden supports (Figure 34) attached to a wooden platform mounted on sawhorses (Figure 35). The supports held the heat pipe in a close-fitting slot while providing a surface normal to the axis of the pipe for positioning the braces. Rests on each side of the heat pipe slot received a pair of braces. When the internal braces were set on the rests and pushed against the heat pipe they were fixed in position against the support with small C-clamps.

The wooden platform rested on sawhorses. Machine screws through the platform provided adjusting legs to level the platform (Figure 36).

### **2.3.2 Radiator Frame Table.**

The radiator frame table held the completed radiator frame in position for attachment of the surface panels. The table was formed with a surface matching the angles of the frame (Figure 37). The table was constructed of plywood with a 0.5 cm layer of foam rubber for cushioning. It rested on sawhorses during use.

### **2.3.3 Panel Pressure Plate.**

Pressure plates were fabricated to apply pressure to the surface panels being attached to the radiator frame. The panels were made of .3 meter by 1.5 meter sheets of plywood with strips of foam rubber attached at the locations where pressure was to be applied to the panel-frame joint. No pressure was applied to the panels between frame members (Figure 38).

### **2.3.4 Panel Radius Forming Tool**

A final tool was made to form the radius in the radiating panels needed to match the heat pipe. An

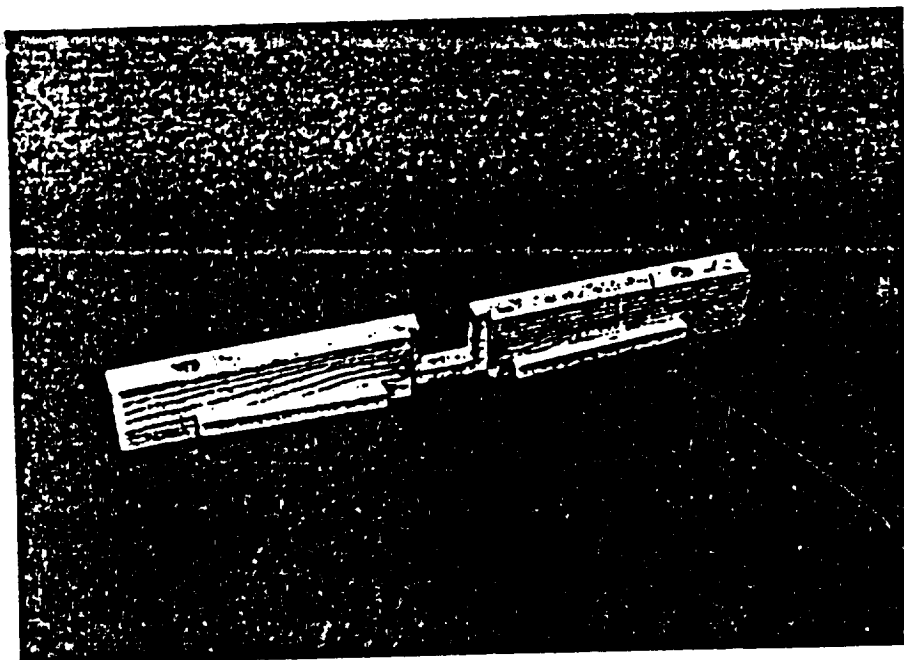


FIGURE 34  
Cradle Support

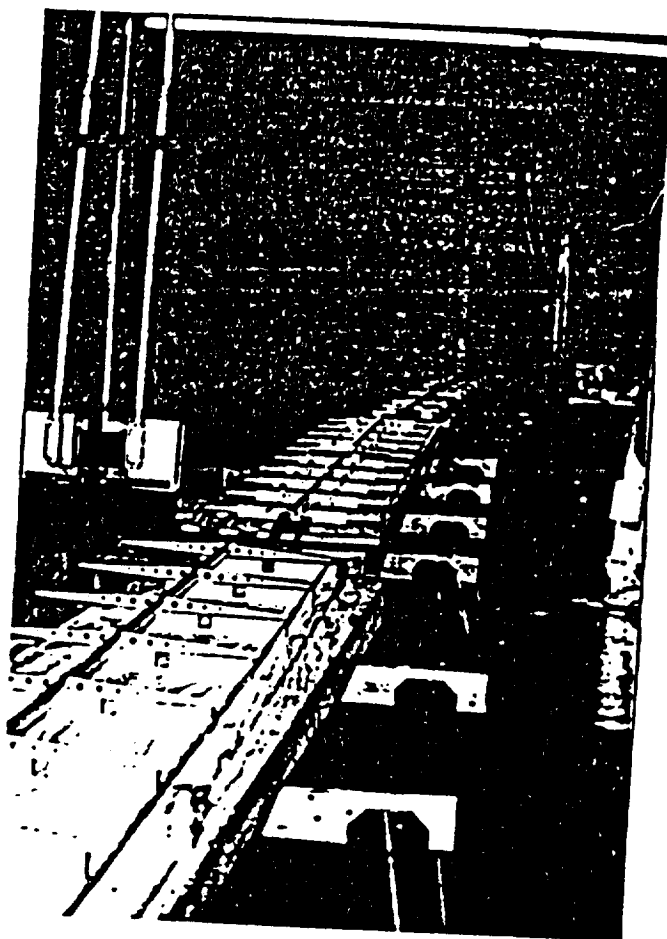


FIGURE 35  
Cradle Platform

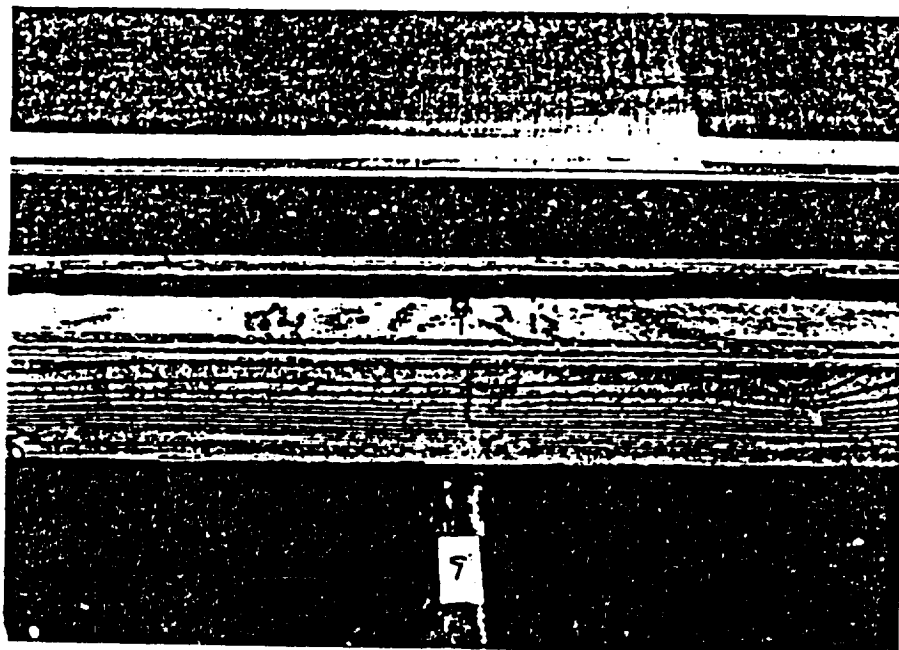


FIGURE 36  
Platform Adjusting Screw



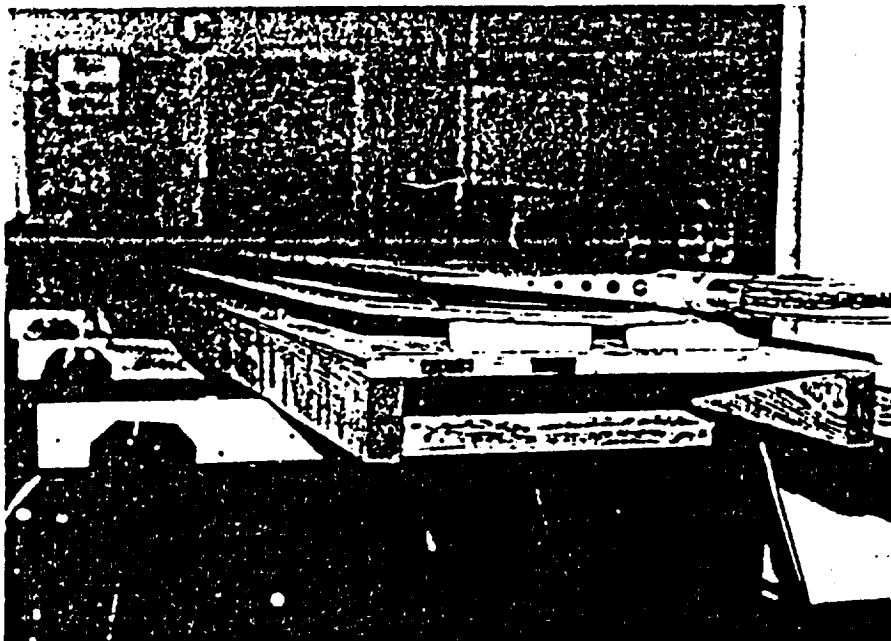


FIGURE 37  
Frame Table

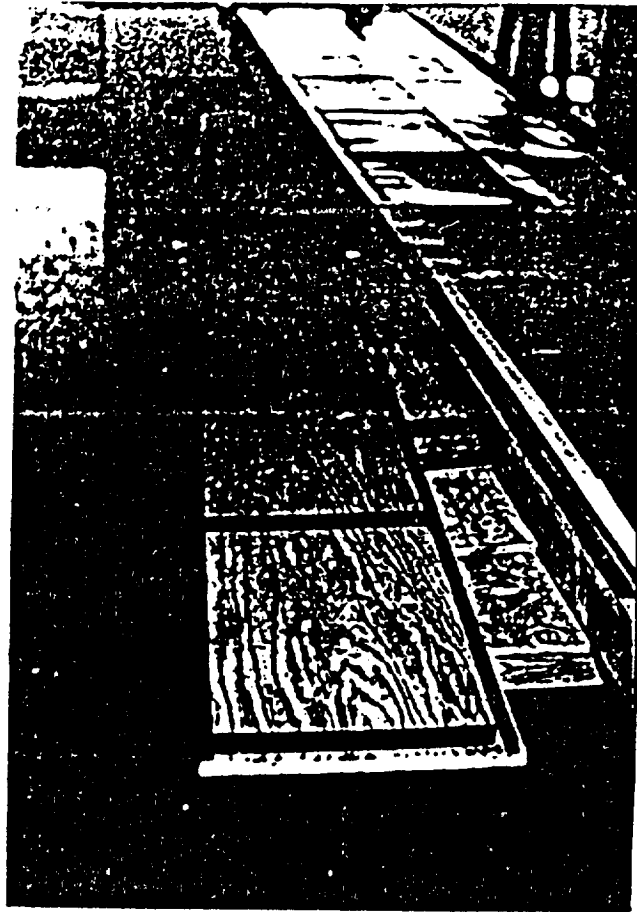


FIGURE 38  
Pressure Plate

oak strip was cut with the appropriate curvature and attached to a plywood platform. Each panel to be formed was clamped against the platform with a length of steel angle. The panel was formed into the radius with a wooded roller. The aluminum-rich area of each panel was ductile enough to permit the forming operation. Springback was sufficiently small that the panels retained a good match with the heat pipe.

#### 2.4 Attach Braces and End-caps to Heat Pipe

Assembly of the radiator frame starts with positioning the heat pipe in the radiator frame cradle (Figure 39). The mating surfaces of each brace and the area of heat pipe surface to which it is to be joined are cleaned with Scotch-brite abrasive and acetone and dried. A film of structural epoxy is spread onto the brace and the brace pressed into position against the heat pipe and the cradle and clamped in position with a C-clamp (Figure 40).

After the epoxy has set (the next day, typically), the end-caps and free ends of the braces are cleaned and epoxy placed on the brace. The end-caps is then pressed onto the brace and adjusted that the braces are parallel and perpendicular to the heat pipe. The loose ends of the end caps are spliced with an aluminum shim (Figure 26).

After all braces and end-caps were in place, the radiator frame was removed from the cradle and placed on the radiator frame table. An additional fillet of adhesive was applied at the intersection of each brace with the heat pipe.

#### 2.5 Attach Graphite-Aluminum Panels to Radiator Frame

The graphite-aluminum panels were trimmed to size as they were applied to the frame. Each panel was sized so that it terminated at the midline of a brace at either end, along the midline of the end-cap on one side and the center of the heat pipe on the other. The planned assembly technique was to apply three panels simultaneously in one pressing. Structural adhesive was to be applied to the braces and end-caps, apply high thermal conductivity filled epoxy to the root of the radiating panels, the panels positioned on the frame and pressed into place with the weighted pressure plate (Figure 41). Following attachment of all the panels, the discontinuities at the braces and along the heat pipe would be spliced with 0.14 mm 6061 aluminum foil ribbon 32 mm wide applied with structural adhesive.

Several variations of this technique were used in assembling the radiator. The first was to assemble by applying a single panel. The result was satisfactory for the first panel applied and the process was repeated, applying two panels simultaneously. The successful two-panel application was followed by a three-panel application. The application was successful but the waviness of the panels was considered excessive (Figure 42).



FIGURE 39  
Heat Pipe in Cradle

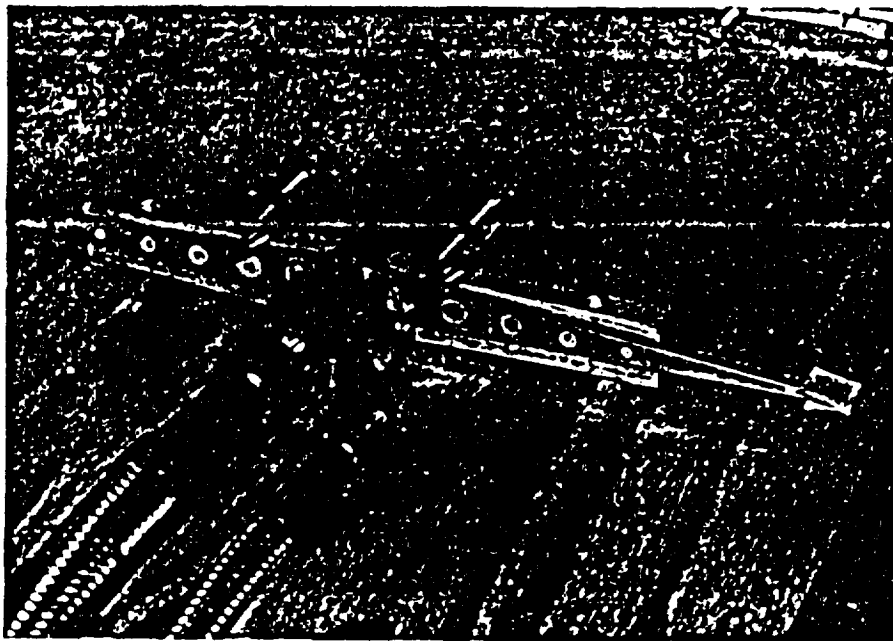


FIGURE 40  
Brace in Position for Bonding

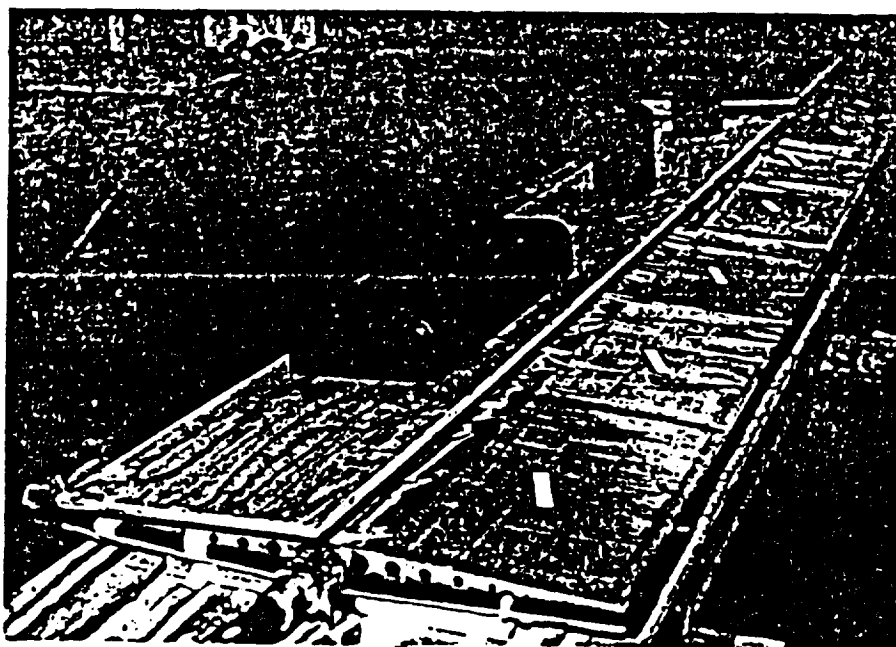


FIGURE 41  
Weighted Pressure Plate

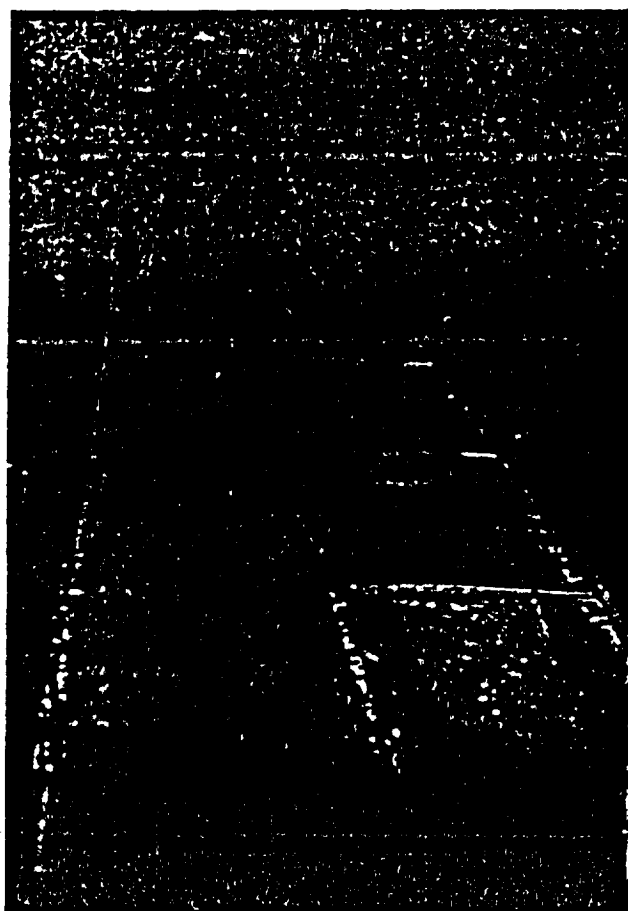


FIGURE 42  
Wavy Panels

In an attempt to reduce the waviness of the next panel applied to the frame, the panel was cut into segments equal in length to the spacing between braces (Figure 43).

Reducing the length of the panel segments did not significantly affect their waviness after mounting to the frame, but did increase the labor required for the assembly. The balance of the panels were applied full-sized, as had been originally planned.

After all the panels had been applied to one side of the radiator, the joints were sanded smooth, cleaned and spliced with aluminum ribbon. A fillet of adhesive was applied to the exposed edge of each panel along the end-cap, further protecting the thin composite. Panels that had been damaged were repaired with an application of aluminum ribbon bonded in place (Figure 44). After one side was completed (panels applied to all three heat pipe segments), the assembly was turned over and the process repeated on the remaining side.

The frame and panels added approximately 1.5 Kg per meter of radiator length (1 pound per foot) to that of the heat pipe alone.

After completion of the radiator, it was carefully folded, packed in its padded shipping crate and sent to NASA JSC.

### 3.0 SUMMARY, CONCLUSIONS AND RECOMMENDATIONS

#### 3.1 Summary

The objective of DWA Composite Specialties, Inc., in this second phase SBIR program was to fabricate a full-scale space radiator built around an experimental folding heat pipe supplied by Thermocore, Inc., of Lancaster, PA. The successful fabrication of the lenticular-section radiator resulted in the largest structure demonstrating the application of high conductivity graphite-aluminum metal-matrix composite material to thermal management.

DWA fabricated the internal support structure around the heat pipe and produced a series of graphite-aluminum panels to be assembled into a lenticular section radiator of monocoque construction. The lenticular section was about 32mm (1.25 inch) deep in the center tapering to about 2mm (.06 inch) at the edges.

The active radiator was approximately 13.5 meters (44 feet) by 0.6 meter (2 feet). MMC surfaces were applied to both sides of the heat pipe. The frame and radiator panels had a mass of 1.5 Kg per meter (1 pound per foot) of radiator length.

The thermal transfer rate per unit mass was optimized by fabricating the MMC radiator skins themselves with a tapered cross section, varying in thickness from 0.63mm (.025 inch) at the center to 0.20mm (.008 inch) at the outer edges. The profile of the taper was the result of an analysis by Dr. Eugene Ungar of NASA Johnson Space Center. The analysis determined the taper required to



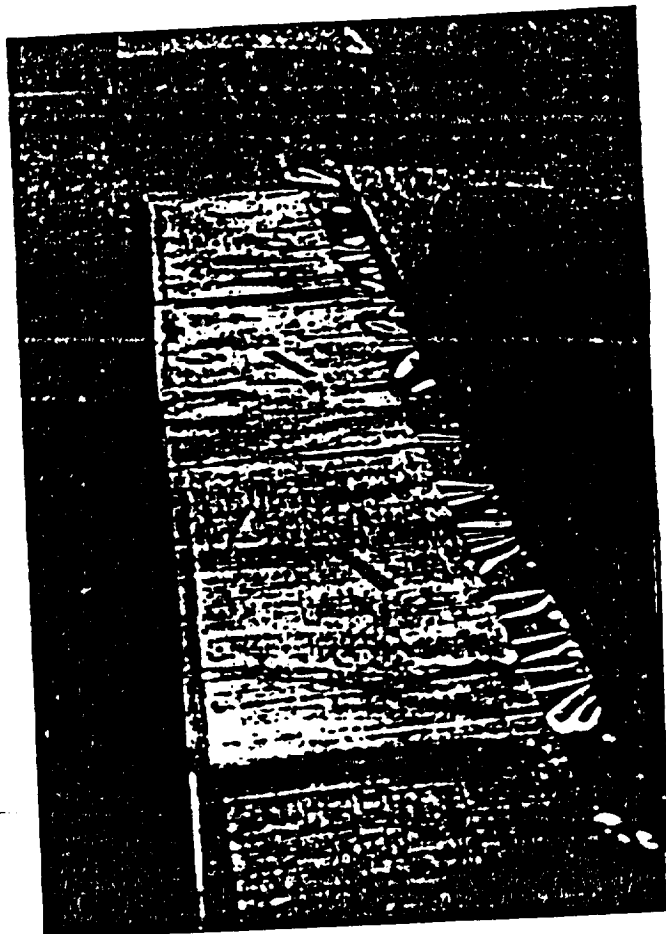


FIGURE 43  
Reduced Length Panels

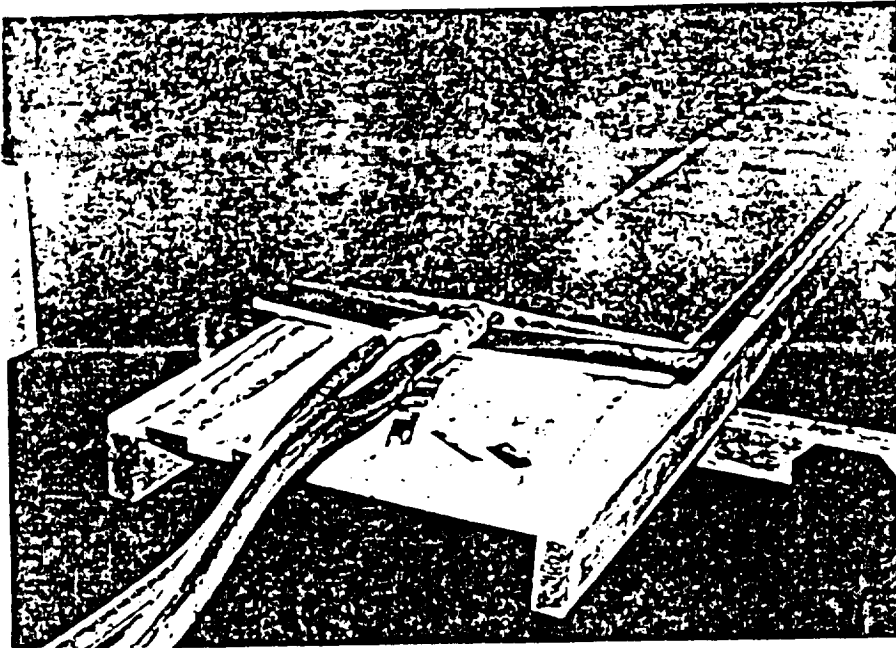


FIGURE 44  
Rubber Repairs

ORIGINAL PAGE IS  
OF POOR QUALITY

maintain a constant thermal flux density through the radiator from the root to the outer edge. His analysis indicated that a 30% weight savings could be achieved without sacrificing thermal transfer rate.

The panels were fabricated by consolidating a set of plies of uniform thickness and varying widths approximating the profile specified by Dr. Ungar. The minimum ply thickness available through DWAs manufacturing process is approximately 0.13mm (.005 inches). The panels therefore consisted of 5 layers of graphite-aluminum stacked to form the required profile. All the graphite in the panels was aligned with the fibers perpendicular to the heat pipe. This orientation of fibers resulted in the maximum thermal conductivity away from the heat pipe.

A set of assembly tools were fabricated and used in the construction of the radiator. After its construction, the radiator was shipped to NASA Johnson Space Center.

In addition to the construction of the radiator, a series of thermal transfer performance and thermal conductivity measurements were made. DWA constructed a small thermo-vacuum chamber with a liquid nitrogen-cooled cold wall. Six specimens were tested: copper, aluminum, tapered unidirectional graphite-aluminum, constant thickness unidirectional graphite-aluminum (in both orientations), 0-90 cross-plyed graphite-aluminum and  $\pm 45$  cross-plyed graphite-aluminum. The thermal conductivity of the same materials was measured. For the anisotropic composite materials, the conductivity was measured in three orthogonal directions.

Of the six panels tested, the highest transfer rate per unit of mass in the given geometry was provided by the tapered graphite aluminum at 186 watts per Kg. The lowest was copper at 12 watts per Kg.

### **3.2 Conclusions**

The unanswered questions at the start of this program were

- 1, was metal matrix composite manufacturing technology sufficiently developed to fabricate a full-sized space station prototype radiator,
- 2, what would be the cost and performance characteristics of such a radiator and
- 3, what would be the minimum weight of a completed 2000-watt space station radiator.

### 3.2.1 Manufacturing Technology

Based on the manufacturing experience gained in this project, the answer to question number one is yes, the current level of manufacturing technology is sufficient for the production of full-sized space station radiators. Including the time to develop fabrication techniques for the tapered panels, the manufacture of the first radiator was accomplished in less than a year. In a production mode, fabrication of a radiator should take approximately 15 weeks from the start of panel production to delivery.

The yield rate of the tapered panels was very good, less than 40 panels were attempted in producing the 36 panels and 2 spares.

The current limit to panel size (using existing tooling) is approximately 2 meters (79 inches) by 0.6 meters.

Internal structure can be made from low cost conventional aluminum using conventional punch-and-form technology.

Some adjustments will be made to the practices used to fabricate this prototype radiator. Eliminating the round heat pipe section will remove the need to provide curved Gr-Al panels and the concomitant need for the aluminum-rich zone. Eliminating this heterogeneity in the material configuration should reduce the waviness in the panels.

We will also select a more suitable adhesive. The system used in this radiator was one we have used in structures intended for space applications. It was thick and difficult to apply properly in this application.

### 3.2.2 Radiator Cost

Based on the cost of fabricating the current radiator, we estimate that the delivered cost to NASA of a production radiator 15 meters long, 0.6 meters wide with radiating panels on both sides would be approximately \$100,000.

The assumptions included in this estimate are

- the heat pipe is supplied by NASA,
- a brief manufacturing technology program detailing fabrication procedures is prior to production,
- labor required is largely technician with little engineering needed
- a heat pipe more amenable to the attachment of panels is developed,
- the surface conversion process is perfected and is applied,
- a satisfactory production NDE process is developed and

- assembly techniques similar to those used to fabricate the current radiator are acceptable.

### 3.2.3 Radiator Weight

The radiating structure designed and fabricated for this project had a mass of 23 Kg (50 lb weight) in excess of the heat pipe alone. This corresponds to a linear mass density of 1.5 Kg per meter of radiator length or one pound of radiator weight per foot. The mass or weight of the heat pipe would be added to this amount. An estimate of the weight of an all-aluminum radiator having comparable thermal transfer capability can be made assuming a constant aluminum panel thickness (3.6/1.9) times the thickness of the composite panel. (The multiplier is the ratio of thermal conductivities of the composite and aluminum). The set of resulting radiator panels would have a mass of 62 Kg (132 lb), 39 Kg (82 pounds) more than the composite. It would appear that the weight savings would reduce launch costs (variously quoted in the thousands of dollars per pound) more than enough to pay for the radiators.

### 3.3 Recommendations

It appears that the high thermal transfer capacity and low mass of the composite radiator has the possibility of significantly affecting the performance and cost of the space station thermal management system. We feel it would be in the best interest of NASA's space station effort to produce at least one production-mode radiator, using the key lessons learned in assembling the prototype and testable in NASA's thermovacuum facility.

The radiator produced on this effort is sufficient for some testing. There are, however, three factors associated with it that could add uncertainty to conclusions drawn from test results.

1. The folding heatpipe was an experimental design with a geometry that made the attachment of radiator panels difficult.
2. The heat pipe was breached during shipment to DWA and was exposed to normal atmosphere for an undetermined period. It is possible that reactions between the components of the air and the sintered aluminum heat pipe interior could have resulted in products that would interfere with capillary flow of working fluid when the heat pipe is recharged.
3. The surface conversion was omitted from the radiating panels. The weight of surface preparations to be added to the radiator to adjust the surface absorptivity and emissivity have not been included

in the radiator weight. It is likely that such preparations could add several pounds to the radiator weight. The anodic surface conversion, however, would not increase it significantly.

To resolve these issues, we recommend the production of from one to five radiators, to be built around NASA-supplied heat pipes. It would be anticipated that the costs of the radiators themselves would approximate the \$100,000 cost referenced above.

The radiators would be of the lenticular section previously demonstrated and employ tapered panels. The effort would include the development and demonstration of the anodic surface conversion for full-sized panels and the development of NDE and QA/QC provisions suitable for production applications.

It would be important to provide heat pipes with flats for the attachment of radiator panels, rather than engineering a panel to be compatible with a round heat pipe.

It would also be possible to consider alternate radiator designs. The radiator built on this program was part of a thermal management design employing free-standing radiators. There has been some concern expressed by those studying the structural requirements of the space station that such radiators would be exposed to stray exhaust from space vehicles maneuvering in its vicinity. The forces exerted on the radiators by such exhaust could generate very large loads and moments on the surrounding structure. Panels could be designed to be attached to the space station truss itself as body-mounted radiators, supported around the perimeter and thus reducing the potential for structural damage due to external loads.

Consideration should also be given to stiffening the basic heat pipe design for vibrational properties and for ease of handling. The heat pipe supplied for this effort was very pliable, flexing to the point of plastic deformation very easily. Not only was handling it without bending it difficult, but it made it impossible to meet the vibrational requirement with a lightweight structure.

Particulate-reinforced aluminum composites could be used in the fabrication of a heat pipe to significantly increase its stiffness. The modulus of elasticity of the composite can be more than double that of the aluminum matrix itself. If suitable designs are available, heat pipes could be made nearly twice as stiff, improving their handlability and increasing their resonant frequency without significantly increasing their weight.

We feel that the success of this program demonstrates the potential for fabricating light-weight radiators with high thermal transfer characteristics at a cost low enough to be offset by savings in the launch cost of the thermal management system.

## APPENDIX 1

### Vibration in Composite Beams

ORIGINAL PAGE IS  
OF POOR QUALITY

## Vibrations in Composite Beams

Allowed transverse vibrations in a clamped-free beam (Figure 1) of uniform section are given by Equation 1<sup>1</sup>.

$$f = \frac{\pi^2 c k^2}{8L^2} (1.194^2, 2.988^2, 5.7^2, \dots) \quad [1]$$

where  $c$  is the wave velocity given by

$$c = (E/\rho)^{1/2}$$

$k$  is the sectional radius of gyration given by

$$k = (I/A)^{1/2}$$

where  $E$  is the modulus of the beam parallel to its length.

$\rho$  is the density.

$I$  is the beam moment of inertia relative to the neutral or bending axis.

$A$  is the sectional area of the beam.

and  $L$  is the beam length.

The constants  $(1.194^2, 2.988^2, 5.7^2, \dots)$  apply to the first, second, third resonant mode, etc.

Equation 1, as shown applies only to homogeneous beams. To calculate the resonant frequencies of composite beams, adjustments must be made, substituting  $E_c$  for  $E$ ,  $\rho_c$  for  $\rho$  and  $I_c$  for  $I$ , where the subscript "c" refers to overall effective properties of the composite beam.

### Neutral Axis

Calculation of the moment of inertia of the beam is made relative to the bending or neutral axis of the beam. Elements on one side of this axis experience compressive stresses, elements on the opposite side experience tensile loads. The first step in determining the overall moment of inertia is to locate the neutral axis.

Given a beam of arbitrary section (Figure 2), exhibiting a modulus that varies with  $y$  (but not  $x$ ), equilibrium at any section through the beam requires

$$\int \sigma(y) dA = 0$$

or

$$\int E(y) \epsilon(y) dA = 0.$$

---

1. Kinsler and Frey, Fundamentals of Acoustics, Wiley & Sons, p76



In a beam undergoing small deflections, the strain at any point is proportional only to its distance from the neutral axis, and not on material properties,

$$\int E(y) \alpha (y - y_b) dA = 0$$

where  $\alpha$  is a proportionality constant. The constant can be factored out and eliminated by dividing through by  $\alpha$ .

If the assumption is made that the material possesses properties that are constant over discrete intervals of  $y$ , the integral can be divided into the sum of several integrals, the modulus being constant over each:

$$E_1 \int (y - y_b) dA = 0.$$

Recognizing that

$$\int y dA = Y_c$$

where  $Y_c$  is the  $y$  coordinate of the centroid of an area, this can be expressed as:

$$\sum E_1 A_1 (Y_{c1} - y_b) = 0 \quad [2]$$

where  $E_1$  is the modulus of the  $i^{\text{th}}$  layer of the beam,

$A_1$  is the sectional area of the  $i^{\text{th}}$  layer,

and  $Y_{c1}$  is the  $y$  coordinate of the sectional centroid of the  $i^{\text{th}}$  layer.

The neutral axis of the composite beam is located at  $y_b$  satisfying Equation 2.

### Moment of Inertia

The overall moment of inertia of the composite beam is calculated relative to the neutral axis just established. Using the Parallel Axis Theorem, the moments of inertia of each element of the beam are summed:

$$I_0 = I_1 + A_1 (Y_{c1} - y_b)^2 \quad [3]$$

where  $I_0$  is the overall moment of inertia,

$I_1$  is the sectional moment of inertia of each layer of the beam, measured relative to an axis through its centroid parallel to the neutral axis of the beam,

$A_1$  is the sectional area of each layer of the beam,

$Y_{c1}$  is the  $y$  coordinate of the centroid of each sectional area

and  $y_b$  is the  $y$  coordinate of the beam's neutral axis.

ORIGINAL PAGE IS  
OF POOR QUALITY

The fractional contribution of each layer to the overall moment (its moment fraction) is given by:

$$I_1 = \frac{I_1 + A_1 (Y_{c1} - Y_b)^2}{I_0}$$

### Modulus

In general, the bending moment in a beam is given by:

$$M = \int \sigma y dA$$

or

$$M = \int \epsilon E y dA.$$

Assuming  $\epsilon$  is proportional to  $y$  (measured from the neutral axis), and  $E$  is constant over beam, the expression for the bending moment simplifies to:

$$M = \alpha E \int y^2 dA_1 \quad [4]$$

$$= \alpha E I_0. \quad [5]$$

If the beam is formed of materials with varying  $E$ , such that  $E$  is constant over discrete intervals of  $y$ , Equation 4 can be written as

$$M = \alpha \sum E_1 \int y^2 dA_1$$

$$= \alpha \sum E_1 (I_1 + A_1 Y_{c1}^2).$$

Comparing this expression to Equation 5, we see that if we define  $E_{eff}$  to be the effective overall modulus of the beam in bending and  $I_0$  to be the overall moment of inertia, the two expressions are equivalent if

$$E_{eff} I_0 = \sum E_1 (I_1 + A_1 Y_{c1}^2)$$

or

$$E_{eff} = \sum E_1 I_1. \quad [7]$$

where  $I_1$  is the moment fraction defined above. This is a rule-of-mixtures formula, analogous expression to those used to calculate the densities, moduli and other properties of mixed systems.

### Density

The overall density of a composite system is given by:

$$\rho_0 = \sum \rho_1 v_1$$

where  $\rho_1$  is the density of the  $i^{th}$  component

and  $v_1$  is the volume fraction of the  $i^{th}$  component.

ORIGINAL PAGE IS  
OF POOR QUALITY

In a system where the configuration is constant in one direction, such as the beams under consideration, the volume fraction is equal to the area fraction of each component:

$$v_i = a_i = A_i / A_{\text{total}}$$

where  $A_i$  is the sectional area of the  $i^{\text{th}}$  component, and

$A_{\text{total}}$  is the overall area.

The effective density of beam is then given by

$$\rho_0 = \sum \rho_i a_i \quad [8]$$

#### Resonant Frequencies of Vibrating Composite Beams

Rewriting Equation 1, using the effective modulus, moment of inertia, density and sectional area of the composite beam in place of the same properties in the homogeneous case, we have for the lowest resonant frequency.

$$r = \frac{\pi}{8L^2} \sqrt{\frac{E_{\text{eff}} I_0}{\rho_0 A}} \quad (1.194^2) \quad [9]$$

#### Example: Vibrations in Composite Radiator Panels

Consider a radiator consisting of a heatpipe bonded to a single planar radiating panel, shown in Figure 2. The heatpipe is aluminum with density 2710 Kg/m<sup>3</sup> and modulus 6.820 X 10<sup>10</sup> Pa. Three panels will be considered: plain aluminum (properties equal to those given for the heatpipe), aluminum reinforced with longitudinal graphite fibers (running in the long direction of the panel) with modulus 37.51 X 10<sup>10</sup> Pa and density 2572 Kg/m<sup>3</sup>, and a panel of aluminum reinforced with transverse graphite fibers, modulus 4.774 X 10<sup>10</sup> Pa and density 2572 kg/m<sup>3</sup>. The lowest resonant frequency for each will be calculated.

Using the geometries of the heat pipe section and the panel section, we find for all cases

$Y_{c, \text{heatpipe}}$	= .01613 m	(Y centroid of heatpipe section)
$A_{\text{heatpipe}}$	= 2.219 X 10 <sup>-4</sup> m <sup>2</sup>	(area of heatpipe section)
$I_{c, \text{heatpipe}}$	= 3.280 X 10 <sup>-8</sup> m <sup>4</sup>	(sectional moment of inertia of the heatpipe relative to centroid axis)
$Y_{c, \text{panel}}$	= .0309 m	(Y centroid of panel section)
$A_{\text{panel}}$	= 2.323 X 10 <sup>-4</sup> m <sup>2</sup>	(area of panel section)

$$I_{c, \text{panel}} = 1.124 \times 10^{-11} \text{ m}^4 \quad (\text{sectional moment of panel relative to centroid axis})$$

$$\text{Overall area} = 4.542 \times 10^{-4} \text{ m}^2$$

### Aluminum Panel

Neutral Axis -

$$\sum E_i A_i (y_{c_i} - y_b) = 0 \quad \text{Eqn. 2}$$

$$6.820 \times 10^{10} = 2.219 \times 10^{-4} \cdot (.0163 - y_b) +$$

$$6.820 \times 10^{10} = 2.323 \times 10^{-4} \cdot (.0309 - y_b) = 0$$

$$y_b = .0242 \text{ m}$$

Moment of Inertia -

$$I_0 = I_1 + A_1 (y_{c_1} - y_b)^2 \quad \text{Eqn. 3}$$

$$= 3.280 \times 10^{-8} + 2.219 \times 10^{-4} \cdot (.0163 - .0242)^2 + 1.124 \times 10^{-11} + 2.323 \times 10^{-4} \cdot (.0309 - .0242)^2$$

$$= 4.725 \times 10^{-8} + 1.044 \times 10^{-8}$$

$$= 5.769 \times 10^{-8} \text{ m}^4$$

$$i_{\text{panel}} = 1.044 / 5.769 = .181$$

$$i_{\text{heatpipe}} = 4.725 / 5.769 = .819$$

Effective Modulus -

$$E_{\text{eff}} = \frac{\sum E_i i_i}{\sum i_i} \quad \text{Eqn. 7}$$

$$= \frac{6.820 \times 10^{10} \cdot .181 + 6.820 \times 10^{10} \cdot .819}{.181 + .819}$$

$$= 6.820 \times 10^{10} \quad (\text{for a homogeneous case, the effective modulus equals the homogeneous modulus})$$

Overall density -

$$\rho_o = \frac{\sum \rho_i A_i}{\sum A_i} \quad \text{Eqn. 8}$$

$$= 2710 \cdot \frac{2.219 \times 10^{-4}}{4.545 \times 10^{-4}} + 2710 \cdot \frac{2.323 \times 10^{-4}}{4.545 \times 10^{-4}}$$

$$= 2710 \text{ kg/m}^3$$

(for a homogeneous case, the overall density equals the homogeneous density)

Resonant Frequency -

$$f = \frac{\pi}{8L^2} \sqrt{\frac{E_{eff} I_0}{\rho_0 A}} (1.194^2). \quad \text{Eqn. 9}$$

For a radiator 50 ft (15.2 meters) long this yields

$$\frac{\pi}{8(15.2)^2} \sqrt{\frac{6.820 \times 10^{10}}{2710} - \frac{6.769 \times 10^{-8}}{4.542 \times 10^{-4}}} (1.194^2)$$

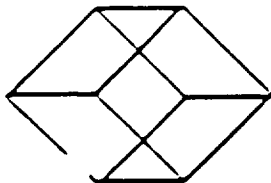
$$f_0 = 0.137 \text{ Hz}$$

Similar calculations using the properties of the graphite-aluminum composite panel in place of the aluminum panel yield:

$$f_{0, \text{long}} = 0.158 \text{ Hz}$$

and  $f_{0, \text{trans}} = 0.130 \text{ Hz}.$

Each of these three cases satisfy the requirement for 0.1 Hz minimum resonant frequency.



## DIELECTRIC MATERIALS

TECHNICAL BULLETIN 3-2-5

ECCOBOND SOLDER 56C

Low Resistance Conductive Cement

Emerson &amp; Cuming

Cemex and Alloy Chemical Division

W. R. Grace &amp; Co.

Canton, Massachusetts 02021 U.S.A.

Telephone (617) 828-3300

Eccobond Solder 56C is a plastic adhesive which when cured has extremely low electrical resistance. It can be cured at temperatures as low as 120°F (49°C) in 2 hours or in a matter of a few minutes at elevated temperature. Supplied in paste form, the adhesive will not flow when applied. It bonds tenaciously to metal, glass, ceramic and plastics. It is used for making electrical connections where wet soldering is impractical, for example, to nichrome wire, or conductive plastics and at locations which cannot be subjected to high temperature. The Catalyst 11 cure results in optimum high temperature properties but gives somewhat poorer electrical conductivity. Eccobond 56C is silver colored. (Note: Eccobond Solder 57C, Technical Bulletin 3-2-5D, can be cured completely at room temperature. In addition, Emerson & Cuming, Inc. has several other conductive adhesives.) Shelf life is at least 6 months when stored in a closed, well-sealed container at temperatures below 25°C.

Thinning of Eccobond 56C with a small amount of toluene (10% by weight maximum) has been used where a thin film is applied. Solvent must be evaporated to assure low resistance. The solvent can be added to the catalyst for ease of use.

Typical Properties:

Temperature Range of Use	-70°F to +350°F (-57°C to 177°C)
Lap Shear Strength, psi (Kg/cm <sup>2</sup> )	800 (54)
Tensile Strength, psi (Kg/cm <sup>2</sup> )	12,200 (857)
Volume Resistance, ohm-cm	2 x 10 <sup>-4</sup>
Thermal Conductivity, (BTU)(in)/(sq)(ft <sup>2</sup> )(°F)	46
Thermal Expansion, /°F (1/°C)	(0.014)
	20 x 10 <sup>-6</sup> (36 x 10 <sup>-6</sup> )

The handling of this product should present no problems if ordinary care is exercised to avoid breathing vapors, if the skin is protected against contamination, if swallowing is avoided, and if the eyes are protected. We recommend observing the precautions in Public Health Service Publication No. 1040, May 1963, which is available from the Superintendent of Documents, U. S. Government Printing Office, Washington D. C. 20402.

This information, while believed to be completely reliable, is not to be taken as warranty for which we assume legal responsibility nor as permission or recommendation to practice any patented invention without license. It is offered for consideration, investigation, and verification.

Revised 9-10-74

Instructions:

Items to be bonded should be clean. To prevent adhesion use Mold Release 1225.

1. Weigh out the amount of adhesive required. Use 1 part Catalyst 9 to 40 parts Eccobond Solder 56C by weight. A medicine dropper provides a convenient method of measurement of catalyst. Use one drop of Catalyst 9 for each gram of Eccobond Solder 56C. Mix very thoroughly.
2. Apply to surface to be bonded. No pressure is required. Cure takes place within 2 hours at 120°F (49°C), but can be accomplished within a few minutes at 150°F to 200°F (66°C to 93°C). Cure at a temperature of 150°F (66°C) or above is preferred for low resistivity.
3. For longer "pot life" and optimum high temperature properties use one part Catalyst 11 to 30 parts of Eccobond Solder 56C or 1-1/2 drops of Catalyst 11 per gram of adhesive. Mix very thoroughly. Cure for 8 hours at 170°F (77°C) or 1 hour at 250°F (121°C).

Printed in U. S. A.

## APPENDIX 2

### High Thermal Conductivity Filled Epoxy

ORIGINAL PAGE  
OF POOR QUALITY

## APPENDIX 3

### Structural Epoxy

ORIGINAL PAGE IS  
OF POOR QUALITY



**M&T**  
**CHEMICALS INC.**

FUNCTIONAL PLASTICS DIVISION

501 SAN FERNANDO ROAD WEST  
LOS ANGELES, CALIFORNIA 90039  
247-6270  
TWX (90) 697-2060

**FURANE<sup>®</sup> PRODUCTS**

**INFORMATION SHEET**

**EPIBOND<sup>®</sup> 1210**

**General Purpose Adhesive**

**EP-58-23-G-0**

**DESCRIPTION:** EPIBOND<sup>®</sup> 1210 may be combined with various hardeners to bond metal, plastics, wood and related products. Because of its semi-fluid consistency, it is well suited to applications by spatula, brush, or dispensing units. Chief among its attributes though, is its ability to bond well to so many diverse materials.

**PREPARATORY MEASURES:** Surfaces to be bonded should be clean and thoroughly degreased. Best bond strengths on metal surfaces are obtained when metal is chemically cleaned. For further information see Surface Preparation Bulletin EP-56-10.

**HARDENER SELECTION:** EPIBOND<sup>®</sup> 1210-B - Long working life, thick fluid mixture. By varying ratio, softer or harder cured adhesive can be achieved. Increase the quantity of hardener in mix to gain softer, more flexible adhesive.

Hardener 9615-A - Long working life, thixotropic paste mixture. Can be varied in ratio with resin as with Hardener 9615.

Hardener 9861 - Shorter working life, but yields higher bond strengths at 200-300°F. (93-150°C.).

**MIX RATIO:** To 100 parts by weight of EPIBOND<sup>®</sup> 1210, add  
65 parts by weight of EPIBOND<sup>®</sup> 1210-B (or equal parts by volume).

To 100 parts by weight of EPIBOND<sup>®</sup> 1210, add  
65 parts by weight of Hardener 9615-A (or equal parts by volume).

To 100 parts by weight of EPIBOND<sup>®</sup> 1210, add  
20 parts by weight of Hardener 9861.

**POT LIFE:** At room temperature (77°F. or 25°C.) two pounds of resin/hardener mixture will have a pot life of:

1210-A/1210-B	50-75 minutes
1210/9615-A	50-75 minutes
1210/9861	35-60 minutes

\*Registered U.S. Patent Office

Page 1 of 2 pages.

FOR INDUSTRIAL USE ONLY. M&T Chemicals Inc. gives no warranty, express or implied, and all products are sold upon condition that purchasers will make their own tests to determine the quality and suitability of the product. M&T Chemicals Inc. shall be in no way responsible for the proper use and service of the product. Any information or suggestions given are without warranty of any kind and purchasers are solely responsible for any loss arising from the use of such information or suggestions. No information or suggestions given by us shall be a recommendation to use any product in conflict with any existing patent rights.

**CURE:** 48 hours at 75-80°F. (24-27°C.), OR  
2 hours at 150°F. (66°C.) required for full cure.

**TYPICAL PHYSICAL PROPERTIES:**

<u>Tests</u>	<u>Results</u>	<u>Test Methods</u>
<u>EPIBOND 1210-A/B or 9615-A</u>		
Lap Shear, psi Aluminum to Aluminum	77°F. 2,500	ASTM-D-1002
Steel to Steel	77°F. 2,500	
Steel to Steel	150°F. 500	
Polyester to Polyester	77°F. 1,800 (failure in laminate not bond line)	
Immersion in tap water, hydraulic oils, gasoline	Negligible effect on lap shear	
Solids content, %	100	
Maximum Service Temperature, °F.	200	

<u>EPIBOND 1210/9861</u>		
Lap Shear, psi Aluminum to Aluminum	77°F. 2,800	ASTM-D-1002
	200°F. 2,500	
	300°F. 500	
Immersion in tap water, hydraulic oils, gasoline, and salt water	Negligible effect on lap shear	
Solids content, %	100	
Maximum Service Temp., °F.	300	

The values shown above are typical and are not recommended for specification purposes unless practical tolerances or limitations are established with M&T Chemical's laboratories.

**STORAGE:** Kept in tightly closed containers, shelf life should be at least one year at room temperature.

**CLEANLINESS AND SAFETY:** Avoid contact of the resin or hardener with the skin and use under conditions of good ventilation. For experimental and production uses of epoxy resins and hardeners, the importance of cleanliness and use of rubber gloves should be emphasized. Request and examine Safety Bulletin EP-54-8.

FOR INDUSTRIAL AND PROFESSIONAL USE ONLY.

**END**

**DATE**

**FILMED**

3 - 5 - 90